Use of a Regional Approach for Long-Term Simulation of Snow Avalanche Regime: a Case Study in the Italian Alps

Authors: Bocchiola, Daniele, Medagliani, Michele, and Rosso, Renzo

Source: Arctic, Antarctic, and Alpine Research, 41(3) : 285-300

Published By: Institute of Arctic and Alpine Research (INSTAAR), University of Colorado

URL: https://doi.org/10.1657/1938-4246-41.3.285

Arctic, Antarctic, and Alpine Research, Vol. 41, No. 3, 2009, pp. 285–300

Use of a Regional Approach for Long-Term Simulation of Snow Avalanche Regime: a Case Study in the Italian Alps

Daniele Bocchiola†*
Michele Medagliani‡ and*
Renzo Rosso§*

*Department of Hydraulic, Roads, Environmental and Surveying Engineering, Politecnico di Milano, L. Da Vinci Square 32, 20133 Milano, Italy
†Corresponding author.
daniele.bocchiola@polimi.it
‡m.medagliani@diiar-idra.polimi.it
§renzo.rosso@polimi.it

Abstract

A method for long-term simulation of snow avalanches is developed, based on coupling statistical interpretation of triggering snowfall process and regional avalanche data. The case study area is the Alta Valtellina region, in the northern Italian Alps. Therein, a 21-year-long series of daily snowfall data from 21 snow stations is used to calibrate a daily point snowfall statistical model. Then, a data set including 68 avalanche events from six historical avalanche sites are used to evaluate regionally valid features of avalanche release probability, geometry, and runout. These findings are then used to set up a model for the occurrence of avalanches. One particular case study site is considered, the Vallecetta mountain, of interest because of the considerable number of avalanche events occurring there. Long-term simulation of daily snowfall is performed, which is then fed into a model of snow avalanche occurrence. Snow avalanche simulations are then carried out, resulting in synthetic statistics of avalanche geometry, volume, and runout for a return period of 300 years. These are compared with regionally observed statistics in the considered area, resulting in acceptable agreement. The proposed model allows long-term simulations of avalanche occurrences for evaluation of snow avalanche volume and runout, usable for ecological and geomorphologic purposes. Integration with an avalanche dynamics model would provide long-term avalanche hazard assessment for land use planning purposes.

DOI: 10.1657/1938-4246-41.3.285

Introduction

Influence of snow avalanches on morphology and ecology of mountain areas is paramount. Snow avalanches redistribute snow mass deposited during winter, considerably affecting snowpack distribution on a local scale (e.g. Elder et al., 1991; Bozhinskiy and Losev, 1998), reducing accumulations on steep slopes (e.g. Elder et al., 1998), and impacting mass balance of snow-covered and glacierized areas (e.g. Kuhn, 2003; Wagnon et al., 2007). While airborne avalanches provide little geomorphic effect (e.g. Bozhinskiy and Losev, 1998; Jomelli and Bertran, 2001), flowing avalanches result in soil removal in the release and flowing zone (e.g. King and Brewster, 1978; Heckmann et al., 2005), removal of shrubs and trees (e.g. Muntán et al., 2004; Casteller et al., 2007; Reardon et al., 2008), sediment transport at the avalanche-to-soil interface (e.g. Jomelli and Bertran, 2001; Schrott et al., 2003), formation of impact pool-mound complexes (e.g. Smith et al., 1994), and modified landforms in alpine areas (e.g. Jomelli and Francou, 2000). Avalanches may influence the erosional features of headwater streams of active river channels, cascading into sediment yield from upper catchments (e.g. Ackroyd, 1987). The frequency and magnitude of avalanches influence soil composition and sediment properties (e.g. De Scally and Owens, 2005), sorting in the flowing and deposition area (e.g. Luckman, 1977; Gardner, 1983; Schaerer, 1988; Bell et al., 1990; Blikra and Sæmundson, 1998; Heckmann et al., 2002; Decaulne and Saemundsson, 2006), and also soil chemical composition (e.g. Freppaz et al., 2006). Due to considerable soil removal on their track, avalanches may result in enhanced soil instability (e.g. Heckmann et al., 2002; Freppaz et al., 2006).

Also, the occurrence and size of snow avalanches affect biophysical diversity (e.g. Geertsema and Pojar, 2007), influence forest structure (e.g. Patten and Knight, 1994; Bebi et al., 2001; Kulakowski et al., 2006) and yield of dead vegetation to streams (e.g. Fetherston et al., 1995; Bartelt and Stöckly, 2001; Benda and Sias, 2003), and also interact with the dynamics of forest fires (e.g. Veblen et al., 1994). Furthermore, the structure and composition of avalanche tracks provide unique habitat for animal and plant species (e.g. Erschbamer, 1989; Mace et al., 1996; Krajick, 1998; McLellan and Hovey, 2001). Accordingly, modeling of flowing avalanche occurrence, volume, and runout and the geomorphologic effect therein is of interest.

The snow depth in the avalanche release zone is often assumed to coincide with the snow depth precipitation in the three days before the event, H_{72} (e.g. Burkard and Salm, 1992). Statistical analysis of H_{72} is therefore used to evaluate snow depth (and volume) at an avalanche start for given return periods (Hopf, 1998; Barbolini et al., 2002, 2003; Ancey et al., 2004; Bocchiola et al., 2006; 2008a). For instance, the *Swiss procedure* (*Sp*; e.g. Salm et al., 1990), adopted with few changes also in Italy (Barbolini et al., 2004), provides mapping criteria for dense snow avalanches with return periods $T = 30$ and $T = 300$ years which uses as an input the T-years value of H_{72} for $T = 30$ and $T = 300$, based on the assumption that the avalanche return period matches that of the triggering snowfall. Accordingly, unusually extreme (i.e. greatest annual) avalanches, i.e. those with high return periods, are of interest. However, estimation of snow mass budget and avalanche driven sediment transport might require the description of avalanche dynamics at a smaller time scale.

1523-0430/09 $7.00

Long-term simulation based on climatic input, either observed or simulated, is widely adopted, for instance to evaluate flood frequency (e.g. Cowpertwait, 1994, 1995; Rahman et al., 2002; Rulli and Rosso, 2002), soil erosion (e.g. Rulli and Rosso, 2005), and even avalanche occurrence aimed at hazard mapping (e.g. Ancey et al., 2004). Here, a regionally valid method for long-term simulation of snow avalanches is proposed and tested.

The index value approach is adopted, which implies that values of a variable that are scaled, i.e. divided by an index value, have identical frequency distributions across all sites within a given homogeneous area, or region. This creates increased sample dimensionality for distribution fitting. This approach was developed in the field of flood hydrology (e.g. De Michele and Rosso, 2001, 2002; Katz et al., 2002; Bocchiola et al., 2003) and was successfully applied, among others, to evaluate H_{72} (e.g. Barbolini et al., 2002; Bocchiola et al., 2006, 2008a) and daily Snow Water Equivalent (herein SWE; e.g. Bocchiola and Rosso, 2007a). Here, the index value approach is tentatively adopted to interpret scarce avalanche data from different sites, so increasing sample dimensionality for model estimation.

The case study area is the Alta Valtellina region in northern Italy, where meteorological data as well as avalanche data from six historical avalanche sites are available (see Bocchiola and Medagliani, 2007; Arena Lo Riggio et al., 2009). A 21-year-long series of daily snowfall data is used to calibrate a statistical model able to simulate daily snowfall. This provides the meteorological factor for triggering of avalanche H_{72} evaluated at the daily scale, H_{72d}. A probabilistic framework, conditioned on the magnitude of H_{72d}, is sketched to trigger avalanche events (e.g. Bozhinskiy and Chernous, 1986; Ancey et al., 2004), based on the findings from the avalanche sites. The geometry of the avalanches, including release depth, width, and length, is interpreted using regional statistical distributions evaluated from the observed data. Then, the avalanche runout needs to be evaluated.

The current approaches to avalanche modeling are mainly aimed at the assessment of runout and flow velocity for hazard mapping (e.g. Salm et al., 1990; Barbolini et al., 2004) and risk assessment (e.g. Keylock and Barbolini, 2001; Fuchs et al., 2004; Fuchs and McAlpin, 2005).

Avalanche runout can be estimated according to two main approaches, i.e. empirical (e.g. McClung et al., 1989; McClung and Mears, 1991) and dynamical (e.g. Barbolini et al., 2000; Salm, 2004). The former include, among others, statistics of extremes based on topographic approaches (e.g. α-β model: Lied and Bakkehøi, 1980; Martinelli, 1986; and the runout ratio: Smith and McClung, 1997; McClung, 2001; Keylock, 2005), and empirical regression against terrain features and avalanche size (e.g. Bovis and Mears, 1976; Gruber and Sardemann, 2003; Maggioni and Gruber, 2003; McClung, 2003). The latter include numerical models, either based on the center of mass hypothesis (e.g. Voellmy, 1955; Perla et al., 1980) or continuous (e.g. Bartelt et al., 1999; Christen et al., 2002; Naaim et al., 2004), also including mass uptake (e.g. Sovilla and Bartelt, 2002; Naaim et al., 2003; Eglit and Demidov, 2005; Sovilla et al., 2006, 2007). Empirical methods often rely on regional calibration (e.g. Lied and Bakkehøi, 1980; McClung and Mears, 1991) based on similar topography, used to increase otherwise scarce sample dimensionality (e.g. Keylock, 2005). Similarly, dynamic models are often calibrated against observed runout (while along-track depth and velocity are seldom available) for a number of avalanche sites inside a climatically and topographically homogeneous region (e.g. Barbolini et al., 2003). Dynamic models usually apply to extreme (i.e. of considerable size, and hence return period) avalanches (e.g. Salm, et al., 1990; Bartelt et al., 1999; Christen et al., 2002), while dynamics of small sized (i.e. more frequent) avalanches, which can contribute significantly to geomorphic action (e.g. Luckman, 1977; Ackroyd, 1987), are generally less investigated. Also, proper validation of dynamic models requires evaluation of along-track depth and velocity, which is not available here (and is generally seldom available). Here, a simple regionally valid rule is found, based on the available avalanche data, to evaluate the runout distance. One particular avalanche site is then considered for model application, the Vallecetta mountain, close to the city of Bormio (Sondrio Province, SO), where a considerable number of historical avalanche data is available and that is of interest because of the considerable avalanche events observed therein (e.g. Riboni et al., 2005; Bocchiola and Rosso, 2007b). Simulation of H_{72d} and occurrence of snow avalanches is performed, resulting in estimates of avalanches with a return period up to $T = 300$. The statistics of the geometry, volume, and track length of the resulting avalanches are then compared with the statistics of the avalanche runout and volume observed in the considered site.

Study Area and Available Database

HISTORICAL RECORDS OF SNOW DEPTH

The study area (Fig. 1a) covers the mountainous area of the Lombardia region, in the central Alpine and pre-Alpine area. In this area, at least 40 snow measurement stations are present (see Bocchiola et al., 2006; Bocchiola and Rosso, 2007b), mainly adopted for avalanche warning purposes. These are property of the Interregional Association for Snow and Avalanches (AINEVA, 33 stations), located at the Snow and Meteorological Center of Lombardia Region in Bormio city (see Fig. 1a) and of the Regional Agency for the Protection of the Environment (ARPA) of the Lombardia region (7 stations, concentrated in Valmalenco, shaded area in Fig. 1a), located in Sondrio city. In a recent study, the authors used daily snowpack H_s data from this network to demonstrate the regional homogeneity of the frequency distribution (i.e. growth curve) of the greatest annual dimensionless values of H_{72}, namely $H_{72}^* = H_{72}/\mu_{H72}$, with μ_{H72} local (at a site) average or index value in the considered area (Bocchiola et al., 2006). Notice that the *Sp* suggests evaluation of H_{72} as the "increase in snowpack depth during a period of 3 consecutive days of snowfall" (e.g. Sovilla, 2002; Barbolini et al., 2004), thus in practice including changes in snowpack density due to settling. For consistency with the *Sp*, here the daily H_s data from one station (Bormio, BOR) are used to evaluate the daily snow depth increase H_d as the daily positive variation in H_s. This is different from what was done by Bocchiola and Rosso (2007a), where daily SWE was evaluated by freshly fallen snow depth H_n and its density ρ_n, the difference being due to snowpack settling. We choose here to model the daily H_d instead of directly modeling H_{72}. This allows us, on one side, to describe the snowfall process at the most intuitive daily scale (i.e. the same as the available data), while, on the other side, this might allow for consideration of snowfall dynamics for avalanche simulation at a different time scale than the three day one (e.g. one day or more), in those cases where the hypothesis of avalanche triggering based on H_{72} would not be accurate (e.g. in the Maritime Alps of France, where H_{48} is used; M. Naaim, personal communication, February 2008). BOR station is the most centered with respect to the considered avalanche sites, and also the closest one to the Vallecetta site, which will be investigated in detail. Also, this snow station shows one of the longest available data sets, because there are daily snow depth data available for 21 years (winter 1986–2006). This site is located at a relatively high altitude (1960 m a.s.l.), as compared

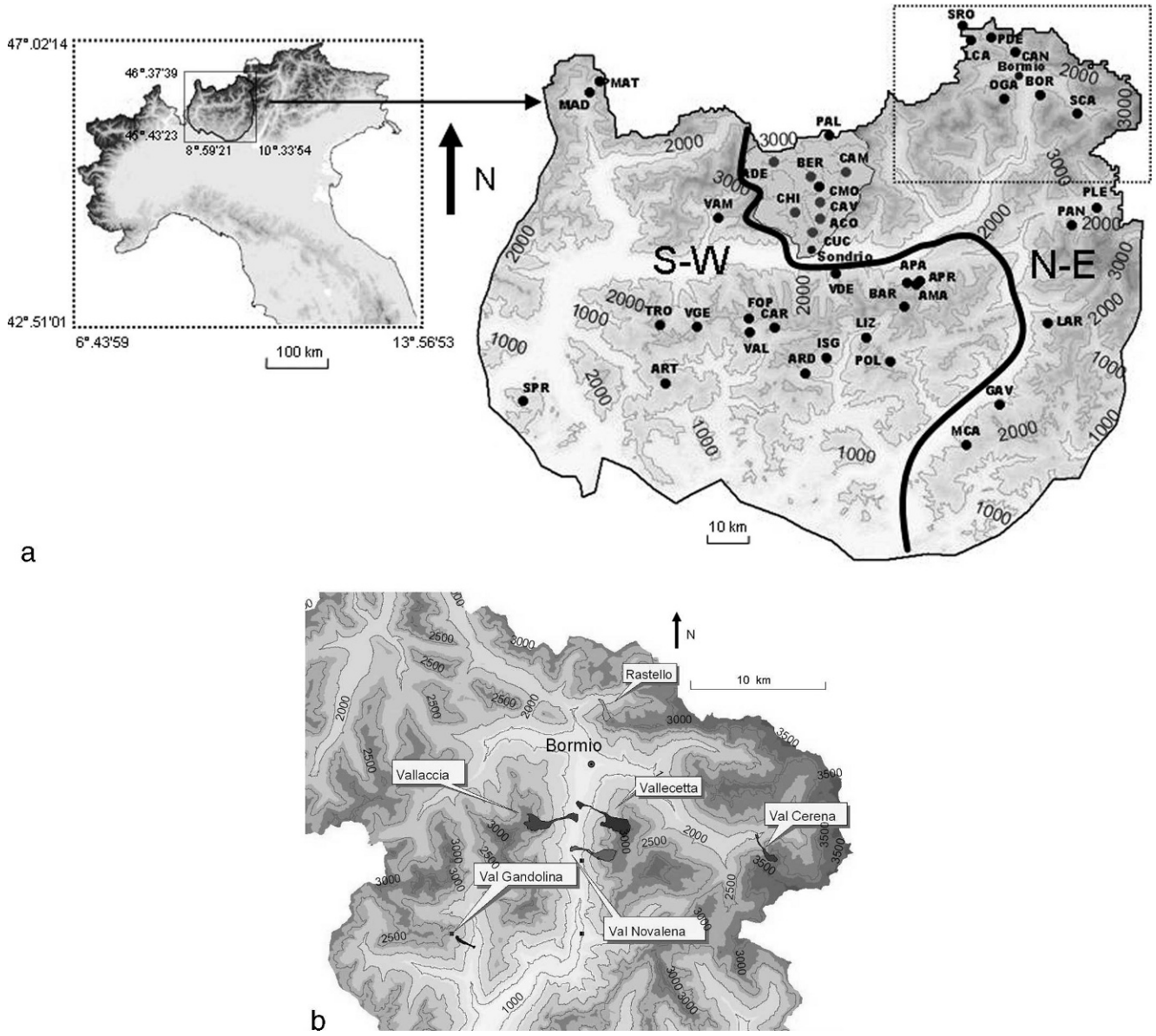

FIGURE 1. (a) Position of Lombardia Region here investigated. The division is showed in N-E and S-W regions. The shaded area is Valmalenco. Dark dots are AINEVA stations, light dots are ARPA stations. See Table 1 for explanation of location abbreviations. (b) Investigated avalanche sites, historical runouts.

with other stations in this area (see e.g. Bocchiola et al., 2006). However, reference control is carried out by considering the data from three other stations, namely Cancano (CAN), Santa Caterina Plaghera (SCA), and Livigno San Rocco (SRO), featuring also 21 years of data each.

Bocchiola and Rosso (2007b) showed that in the investigated region, scaling of the index value μ_{H72} with altitude A shows a less homogeneous behavior than the dimensionless quantiles H_{72}^* (Bocchiola et al., 2006). This occurs because the value of μ_{H72} interprets the local variability of the processes influencing the average magnitude of the observed values of three days snow depth. This issue is often observed in the field of flood hydrology, when regional homogeneity of the growth curve does not necessarily imply homogeneity of the index flood values (i.e., their relationship with geomorphologic attributes, particularly with drainage area), thus requiring a further step in the regionalization procedure (''hierarchic approach'' to regionalization; see Gabriele and Arnell, 1991). Bocchiola and Rosso (2007b), using cluster analysis (CA; see Baeriswyl and Rebetez, 1997), divided the considered region into two sub-regions where homogeneous scaling of μ_{H72} against A is observed, indicated in Figure 1a and referred to as S-W and N-E.

To simulate H_d in the release area of avalanches, usually located at high altitude where no snow gages are available, one can use the dependence of its average value μ_{Hd} upon A (Bocchiola et al., 2008a). In such cases, evaluation of average snow depth from altitude A is reasonable, because A is possibly the factor that mostly influences the distribution of snowfall in space (see e.g. Barbolini et al., 2002, Bocchiola and Rosso, 2007b; Bocchiola et al., 2008a). Because here different scaling of μ_{H72} with A is observed in the two sub-regions S-W and N-E, it is expected that also μ_{Hd} behaves accordingly. Therefore, data of H_d from the 21 available stations in region N-E are also included in the analysis, to evaluate scaling of μ_{Hd} against A.

HISTORICAL RECORDS OF SNOW AVALANCHES

The available avalanche data (Fig. 1b) cover the eastern part of Valtellina Valley. Therein, six historical avalanche sites were investigated for 68 observed avalanche events. The six sites are Val Cerena (herein CER), Val Gandolina (GAN), Val Novalena (NOV), Rastello (RAS), Vallaccia (VCA), and Vallecetta (VCE). Avalanche data were retrieved mainly from the database of the Rangers of Sondrio City (Corpo Forestale dello Stato, CFS) and also from the archives of the Italian Association for Snow and Avalanche (AINEVA). Inside these databases, sparse avalanche events are found dating back to 1886, but more accurately measured in the last 30 years or so (see Bocchiola and Medagliani, 2007). Snow avalanche data included avalanche main cause (i.e. heavy snowfall, rain, and temperature, while anthropic action is not considered as a main cause, but rather as a triggering effect), type of avalanche (e.g. slab, loose, superficial, and bottom), geometry at release (i.e. altitude, fracture depth, release area) (sometimes mapped on a chart at a scale of 1:25,000). In most cases, the area of release is evaluated by remote observation (e.g. use of binoculars). *In situ* measurement is carried out only in case of relevant avalanche size. This introduces some degree of uncertainty in the evaluation of the avalanche geometry. Also, deposition data are reported, including morphology (open slope, channelized, gully, etc.), deposition altitude, deposition geometry (also on a chart at a scale of 1:25,000), and volume. *In situ* measurements are carried out in the deposition area if the avalanche event involves people (or property), while if not, remote assessment usually is carried out. Unfortunately, no measurements are available of the deposited snow density, of interest in evaluating the avalanche type and properties. The presence of avalanche defense structures, including rakes, dikes, wedges, diversion structures, etc., are recorded where available. A summary of the database is reported in Table 1.

Methods: Snow Depth Data

DISTRIBUTION OF DRY AND SNOWY PERIODS

To provide synthetic climatic input for avalanche long-term simulation, the available 21 years (1986–2006) of observed series of daily snowfall at BOR station was used to tune a statistical model (see e.g. Ancey et al., 2004). The winter period was investigated, from 1 November to 30 April, because no noticeable snow precipitation was observed before or after this period in the study area. In this preliminary approach, seasonal (e.g. monthly) difference was not considered, and the snowfall series was treated as homogeneous during winter. In the future, more accurate description could be achieved by seasonal partitioning. First, the duration of dry and snowy periods, τ_d and τ_s, was investigated (e.g. Kottegoda et al., 2000). Analysis of the database resulted in a total of 556 wet and snowy spells, i.e. of 2366 dry (1949) or snowy days (417). First, (linear) correlation analysis was carried out to evaluate the dependence between dry and snowy period duration, which might be included in some cases for precipitation simulation purposes (e.g. Salvadori and De Michele, 2006). For the BOR station, this resulted in negligible correlation ($\rho_{\tau d,\tau s} = 0.05$, not significant for a reference significance level $\alpha = 5\%$). Because no sensible correlation exists, duration of dry and snowy periods can be treated independently for present purposes. Following Kottegoda et al. (2000), a geometric (GE) distribution was tentatively used here for distribution fitting of snowy and dry periods. Use of GE distribution stems from modeling the number of dry and snowy days according to a series of Bernoulli trials, each one with given probability of snowing. In some cases, use of log series (LS) might be recommended for τ_d (e.g. Kottegoda and Rosso, 1997; Kottegoda et al., 2000). Other distributions are suitable for the length of snowy and dry periods, including Exponential (EXP) and Weibull (WE; see e.g. Veneziano et al., 2002). Here the four mentioned distributions were tested for accommodation of both τ_d and τ_s. Concerning τ_d, the GE distribution gave considerably better fit than the WE and EXP, and slightly better than LS (not shown; see Pagani and Sala, 2007). Concerning τ_s, all the proposed distributions gave in practice equivalent fitting. For simplicity and consistency with τ_d, here GE distribution is adopted. The parameters of the mentioned distribution are reported in Table 2. In view of these results, the snowfall process is here modeled as a sequence of snowy and dry periods, with duration independent of each other, and evaluated according to a proper GE distribution. As reported in the section *Historical Records of Snow Depth*, reference control is carried out by considering the data from three other stations, namely CAN, SCA, and SRO. The results reported here concerning τ_d and τ_s for BOR station was found to be in practice equivalent for all four stations. Based on these findings, it is tentatively assumed that the distribution of τ_d and τ_s is valid for the considered region and can be therefore used to simulate snowfall process in the considered avalanche sites.

DISTRIBUTION OF DAILY SNOW DEPTH H_D

First, the dependence between τ_s and cumulated snow depth H_d was tested. In fact, a direct dependence can exist between the two (e.g. Kottegoda et al., 2000; Salvadori and De Michele, 2006); however, no correlation was found therein ($\rho_{Hd\tau s} = 0.02$, not significant for $\alpha = 5\%$). Also, the independence between duration of the dry periods τ_d and subsequent snow depth H_d in the first snowy day (Kottegoda et al., 2000) was verified ($\rho_{Hd\tau d} = -0.04$, not significant for $\alpha = 5\%$). Then, the dependence between H_d in two consecutive snowy days was investigated ($\rho_{Hd,Hd+1} = 0.08$, not significant for $\alpha = 5\%$). Eventually, H_d distribution was evaluated from the available database of 417 events and treated as independent according to these findings. Particularly, the distribution of the H_d values, made dimensionless with respect to their local index value, $H_d^* = H_d/\mu_{Hd}$ was investigated. Distribution fitting of H_d^* is tentatively carried out using GA, LN, WE distribution (e.g. Bocchiola and Rosso, 2007a), and EXP distribution, suitable for precipitation depth (e.g. Bacchi et al., 1994). The best visual fit (see Pagani and Sala, 2007) is given by the GA and WE distribution, while LN and EXP fail to meet the confidence limits according to the Kolmogorov Smirnov goodness of fit test (herein KS; see e.g. Kottegoda and Rosso, 1997) for a level $\alpha = 5\%$. The GA distribution is chosen here (reported in Table 2) because of its frequent use to model rainfall (e.g. Katz, 1999; Wilby and Wigley, 2002) and also daily snow depth H_d (e.g. Skaugen, 1999). Also for H_d^*, reference control is carried out by considering the data from three other stations, namely CAN, SCA, and SRO. The results reported here for BOR station was found to be in practice equivalent for all the four mentioned stations. It is therefore assumed that the distribution of H_d^* is valid for the considered region and can be used to simulate snowfall process in the considered avalanche sites. However, to fully simulate snowfall depth H_d in an unmeasured site, e.g. in the release area of an avalanche, one needs to know the index value μ_{Hd}. Using the daily snow depth database from the 21 snow stations in the N-E region reported in Figure 1a, scaling of μ_{Hd} against altitude A was investigated (Fig. 2). Using weighted (i.e. on their estimation variance, depending upon the number of

TABLE 1

Main features of the selected avalanches. CER—Val Cerena, GAN—Val Gandolina, NOV—Val Novalena, RAS—Rastello, VCA—Vallaccia, VCE—Vallecetta. A_0 is release altitude, h_0 release snow depth, W_0 release width, L_0 release length, S_0 release area, V_0 release volume, A_r altitude at deposition, L runout length, V_r volume at deposition. Bold indicates length and volumes at release that required estimation using GIS and avalanche track maps data to be used in the analysis. Italic indicates volumes that are found to be less accurate and were not used in the evaluation of growth index. Cause indicates snowfall (SF), rainfall (R), or temperature (T) due avalanches. Types, first letter indicates either Slab (S) or Loose (L) avalanches, second letter indicates either Surface (S) or Bottom (B) avalanches. Missing values are cases when either a feature was not measured, or it was not reported in the avalanche forms, or was unintelligible.

ID	Date	A_0 (m asl)	h_0 (m)	W_0 (m)	L_0 (m)	S_0 (ha)	V_0 (m^3)	A_r (m asl)	L (m)	V_r (m^3)	Cause	Type
CER1	?/04/1975	—	—	—	—	—	—	1980	—	—	T	SB
CER2	?/05/1977	2650	1.5	640	**206**	—	**2.00E+05**	1900	1700	—	R	SB
CER3	20/05/78	2600	1.5	350	**205**	—	**1.10E+05**	1920	1800	—	R	SB
CER4	?/02/1979	2600	1	700	**240**	—	**1.70E+05**	1920	1500	—	SF	SS
CER5	23/05/83	—	—	—	—	—	—	1970	—	—	SF	SB
CER6	12/04/86	2670	2	550	18	1	2.00E+04	1930	1880	2.40E+05	SF	SB
CER7	05/04/89	2500	0.4	450	211	9.5	3.80E+04	1920	1350	1.50E+04	SF	L
CER8	21/04/90	2800	1.5	150	20	0.3	4.50E+03	1930	1920	2.00E+04	SF+T	L
CER9	08/03/91	2400	1.2	500	20	1	1.20E+04	1930	1100	1.20E+05	R	L
CER10	06/04/98	2350	0.5	40	50	0.2	1.00E+03	2000	600	1.40E+03	SF	SS
CER11	04/05/99	2700	2	350	29	1	2.00E+04	1920	1870	2.20E+04	R	SS
CER12	17/04/00	2550	0.8	150	287	4.3	3.40E+04	1920	1460	1.20E+04	SF	SS
CER13	16/11/00	2550	1.5	150	333	5	7.50E+04	1920	1460	1.50E+04	SF	SB
CER14	08/01/01	2550	0.6	500	80	4	2.40E+04	1920	1480	1.20E+04	SF	SS
CER15	03/05/02	2550	1.5	350	86	3	4.50E+04	1920	1480	7.00E+03	R	L
GAN1	12/01/76	2000	2	—	—	—	**1.70E+05**	1325	1370	—	SF	SS
GAN2	12/01/77	2000	2	100	**310**	—	**6.20E+04**	1400	1100	—	SF	—
GAN3	28/01/79	1938	2	—	—	—	**7.60E+04**	1340	1150	—	R	SB
GAN4	02/02/85	—	—	—	—	—	—	1350	—	—	—	SS
GAN5	23/04/86	—	—	—	—	—	—	1260	—	—	—	SB
GAN6	09/02/88	2200	0.2	200	**668**	0.5	**2.70E+04**	1300	1700	*4.00E+03*	SF	SS
GAN7	10/01/94	2200	1	80	—	1	1.00E+04	1300	900	1.20E+04	SF	SS
GAN8	17/01/01	2200	1	80	**537**	1	**4.30E+04**	1300	900	4.00E+04	SF	SS
NOV1	?/04/1975	—	—	—	—	—	—	1200	—	—	T	SB
NOV2	24/05/77	2700	2	300	—	—	—	1200	3000	—	R	SB
NOV3	16/05/83	2900	1.2	1000	**689**	—	**8.30E+05**	1000	3600	8.00E+05	SF	SS
NOV4	29/04/86	2550	2	600	**67**	1.2	**8.40E+04**	1137	2750	4.00E+04	T	SB
NOV5	08/02/88	2625	0.8	350	**318**	0.2	**8.90E+04**	1135	2700	2.70E+04	SF	SB
NOV6	10/04/88	2800	1	250	—	0.3		1135	3100	8.00E+03	T	L
NOV7	24/03/91	2725	1.3	700	**246**	0.2	**2.20E+05**	1150	2825	1.90E+05	SF	SB
NOV8	18/11/00	2250	0.6	250	**335**	—	**5.03E+04**	1100	1000	2.20E+04	SF	L
RAS1	??/04/1975	—	—	—	—	—	—	1660	—	—	T	SB
RAS2	21/05/78	2300	2	200	—	—	—	1740	560	—	T	SB
RAS3	28/05/81	—	—	—	—	—	—	1680	—	—	T	SB
RAS4	2?/05/1983	2700	1.4	300	**590**	—	**2.50E+05**	1660	1750	—	SF	SB
RAS5	26/04/86	2420	2	375	—	—	—	1660	1250	1.90E+05	SF	SB
RAS6	08/04/88	2412	1	750	4	0.3	*3.00E+03*	1670	1175	8.40E+04	SF	SS
RAS7	??/??/1991	2200	2	220	23	0.5	1.00E+04	1680	680	1.50E+05	T	SB
RAS8	??/??/1992	2700	—	500	325	0.1	**1.30E+05**	1660	1750	1.20E+05	SF	L
RAS9	11/01/94	2600	0.6	325	**497**	0.3	**9.70E+04**	1660	1250	*4.20E+05*	SF	L
RAS10	29/03/00	—	—	—	—	—	—	1660	—	7.50E+04	SF	SS
VCA1	06/01/19	—	—	—	—	—	—	1150	—	—	SF	SS
VCA2	22/02/77	2050	1.5	150	**96**	—	**2.20E+04**	1150	2000	—	SF	SB
VCA3	31/12/81	—	—	—	—	—	—	1280	—	—	R	SB
VCA4	26/04/86	2470	2	400	23	0.9	1.80E+04	1190	2625	6.60E+04	SF	SB
VCA5	15/02/90	2200	0.8	220	2	0.05	*4.00E+02*	2070	225	3.50E+04	SF	SS
VCE1	21/12/1886	—	—	—	—	—	—	1135	—	—	SF	L
VCE2	16/04/26	—	—	—	—	—	—	1155	—	—	BS	—
VCE3	?/?/1946	—	—	—	—	—	—	1900	—	—	—	SB
VCE4	?/?/1947	—	—	—	—	—	—	1900	—	—	—	SB
VCE5	1?/05/1956	—	—	—	—	—	—	1270	—	—	—	SB
VCE6	1?/05/1958	—	—	—	—	—	—	1200	—	—	—	SB
VCE7	1?/05/1975	—	—	—	—	—	—	1240	—	—	—	SB
VCE8	05/05/77	2800	1.5	700	650	—	—	1600	2900	—	R	SS
VCE9	29/05/81	—	—	—	—	—	—	2125	—	—	—	SB
VCE10	01/05/83	2950	0.9	800	**1110**	—	**8.00E+05**	1170	**4250**	1.00E+06	SF	SS
VCE11	16/05/83	3140	1.3	1300	**1254**	—	**2.00E+06**	1130	**4700**	2.12E+06	SF	SS
VCE12	11/01/86	2675	0.7	350	106	3.7	2.60E+04	2175	800	5.00E+04	SF	SS

TABLE 1

Continued.

ID	Date	A_0 (m asl)	h_0 (m)	W_0 (m)	L_0 (m)	S_0 (ha)	V_0 (m^3)	A_r (m asl)	L (m)	V_r (m^3)	Cause	Type
VCE13	11/01/86	2750	0.7	250	68	1.7	1.20E+04	2100	1250	1.10E+05	SF	SS
VCE14	26/04/86	2325	2	320	19	0.6	1.20E+04	1750	1680	4.50E+04	SF	SB
VCE15	05/04/87	2725	0.5	30	17	0.05	*2.50E+02*	2500	400	6.00E+03	SF	SS
VCE16	30/01/88	2800	0.5	500	12	0.6	*3.00E+03*	2150	1250	3.60E+05	SF	SS
VCE17	28/03/88	2615	0.6	15	7	0.01	*6.00E+01*	2470	270	3.00E+03	SF	L
VCE18	12/02/91	2890	0.7	125	80	1	—	2860	150	1.20E+04	SF	L
VCE19	09/03/91	2525	1	285	28	0.8	8.00E+03	2153	625	1.90E+04	R	L
VCE20	12/03/91	2700	1.4	160	31	0.5	7.00E+03	2300	1000	1.00E+05	SF	SS
VCE21	19/02/95	2900	0.6	30	2	0.006	*3.60E+01*	2775	200	4.50E+03	SF	SS
VCE22	12/03/04	2900	1.5	150	280	—	—	2300	700	5.00E+04	SF	SB

available data) linear regression, a significant dependence of μ_{Hd} upon A was found, as reported in Table 3, in spite of the somewhat low determination coefficient, $R^2 = 0.65$. This method is used to evaluate the index value μ_{Hd} in ungauged avalanche release areas.

DISTRIBUTION OF H_{72}

The distribution of H_{72d} is then evaluated by the sum of H_d on a three day moving window. Notice that because H_d is distributed according to a GA distribution, its three day sum is also distributed as a GA distribution (see e.g. Skaugen, 1999). Bocchiola et al. (2006) investigated the regional distribution of the greatest annual H_{72} for a wider region, including the one here considered, finding in practice a Gumbel (GU) distribution. Also Bocchiola et al. (2008a) provided regional frequency curves for H_{72} for Switzerland, finding a satisfying fitting of the Gumbel distribution for six homogeneous regions out of seven.

This is consistent with the findings here, because the greatest (i.e. extreme) values of a variable displaying GA distribution display in turn a GU distribution (e.g. Kottegoda and Rosso, 1997). Several tests (see Pagani and Sala, 2007) indicated consistent statistics (i.e. statistically equivalent variance and average) of the synthetically simulated series of both H_d and H_{72d} with the observed ones.

TABLE 2

Proposed statistical distributions for snowfall and avalanches. Dist. = distribution; see text for definitions.

Var.	Dist.	Par. 1	Par. 2
Snowfall			
		p	-
τ_d	GE	0.15	-
τ_s	GE	0.67	-
		α	v
H_d*	GA	0.64	0.64
Avalanches			
		A	B
F_0	UN	0	3.9
		μ	σ
A_0*	NR	1	0.06
		α	v
L_0*	GA	0.66	0.66
W_0*	GA	2.16	2.16
		λ	
I_g*	EXP	1.07	-

Figure 3 shows the comparison, of interest for the purpose of extreme avalanche evaluation, of the greatest annual values of H_{72d}, H_{72dmax} in BOR station, against those estimated according to the regional growth curve (Bocchiola et al., 2006), used here because it is more reliable than the single site one for the considered return periods. Also, the locally observed values are reported for comparison. Synthetic simulation of H_{72d} for a period of 195 years is carried out using the Monte Carlo method (see Kottegoda and Rosso, 1997), resulting in an estimated return period of 300 years (according to the plotting position APL, $F = (ord - 0.65)/n_{tot}$, where ord is the ranking position of the particular value of H_{72d} in the sample, ordered in decreasing order of magnitude and $n_{tot} = 195$). To avoid sample effects, particularly for high return periods, 100 repetitions were carried out, for a total of $1.95E^4$ simulated values of H_{72dmax}. Then, the average (i.e. average of 100 values for each return period) plotting position so obtained was put in Figure 3. Apart from some slight underestimation, the synthetic series seems to fit well the regional one, and is well contained inside the confidence limits ($\alpha = 5\%$; see Bocchiola et al., 2006, 2008a, about their evaluation), indicating that the proposed model represents well the snowfall process, also for considerable return periods.

Methods: Avalanche Data

ASSESSMENT OF AVALANCHE DATA

For those avalanche events that were reasonably well mapped, the main avalanche features were evaluated. These are avalanche release altitude A_0 and geometry (greatest width W_0,

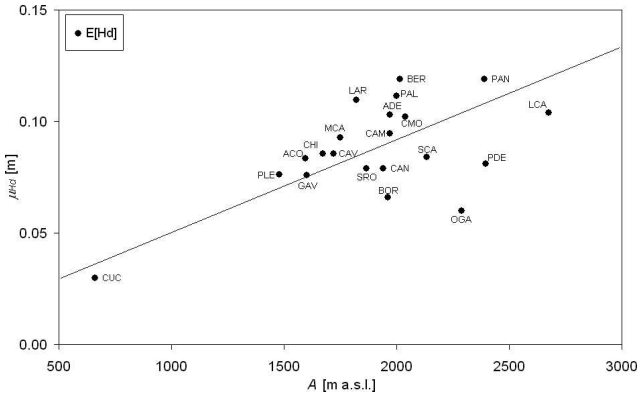

FIGURE 2. Scaling of μ_{Hd} against altitude for stations in region N-E in Figure 1, used here for daily snowfall simulation.

TABLE 3

Proposed regression equations.

Var	Int.	Slope	R^2
A (m a.s.l.)			
μ_{Hd} (m)	$8.7E^{-3}$	$4.16E^{-5}$	0.65
p-val	$1E^{-4}$	$1E^{-4}$	
Log(V_0*) [.]			
Log(L*) [.]	0.089	0.212	0.74
p-val	2E-03	2E-13	

surface S_0, snow depth h_0 at release, and in some cases maps at 1:25,000), and runout altitude A_r, length L, and volume V_r, and in some cases maps at 1:25,000. Frequently, some of the data were missing and therefore several avalanches could not be fully analyzed. A screening was carried out for the presence of manmade structures (walls, rakes, dikes, wedges, diversion structures, etc.) that might have influenced avalanche properties (e.g. release shape or volume, or runout distance, etc.). However, for the studied cases, no considerable influence was observed.

Also, a preliminary screening was carried out to highlight features that are clearly inaccurately estimated. These include erroneous release areas or depth, evaluated e.g. by consistency with released and deposited volume, or erroneous estimates of snow volumes at deposition, evaluated by consistency with snow depth and deposition geometry. Also, GIS-based topographic analysis was carried out to check accuracy of the release and deposition areas and of the indicated topography in the deposition area. This was based on a 20 m cell size DEM of the considered area. The length of the release area L_0 was also calculated, based on the available maps, also verified through topographic analysis. In Table 1 the main avalanche properties are reported, together with a judgment of the quality of the different features. The assessment of the database as here carried out surely implies a degree of subjectivity, but it is deemed to avoid erroneous interpretation of the avalanche process due instead to evident mistakes in data retrieval.

AVALANCHE TRACK GEOMETRY

Figures 4a–4c report the track of the avalanches, including main avalanche profile, track width, and the release and deposition altitude for the avalanche events here mapped. The given profile is the most indicative one, as defined after a preliminary analysis based on dynamic simulation of the greatest (i.e. with the lowest runout altitude) observed avalanche (historical end mark) using a simple dynamic model (Voellmy Salm model, VS; see e.g. Bocchiola and Medagliani, 2007). The six sites show a similar morphology, featuring a wider release area, followed by a channelized flowing zone, and a depositional fan at the valley bottom. The average slope of the release, channelized (i.e. flowing), and deposition, or runout areas, are reported in Table 4. Also, the percentage length of each zone as compared to the whole track length (from the highest altitude to the lowest deposition altitude) is given. Release zone is defined coupling slope analysis (i.e. 30°–60°; e.g. Maggioni and Gruber, 2003) and observed release area. We labeled as flowing area the channelized zone, until start of the alluvial fan. The runout zone is defined between the end of the flowing zone and the historical end mark (i.e. longest runout). The six avalanche sites display reasonably similar values of the slope in the three areas so defined, and also a similar percentage length, as indicated by the corresponding low coefficient of variation CV[.]. This seems to suggest that a similar behavior might be observed in terms of avalanche geometry and runout, provided the proper scale factors are considered (e.g. for

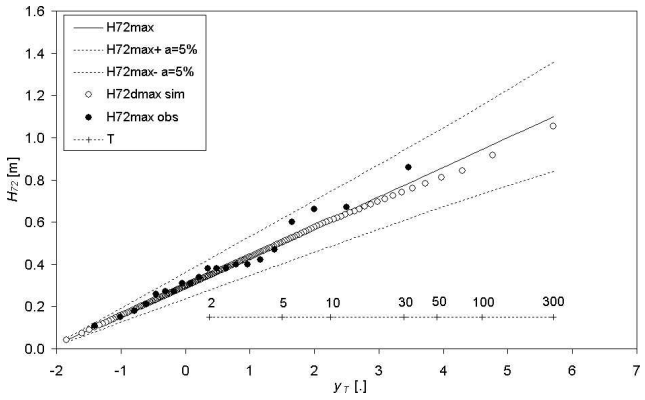

FIGURE 3. BOR station. Greatest simulated annual values of H_{72d}, as compared to observed values and the regionally estimated quantiles. On the x axis the Gumbel dimensionless variable is used, $y_T = -\mathrm{Ln}(\mathrm{Ln}[T/(T-1)])$, with T return period in years.

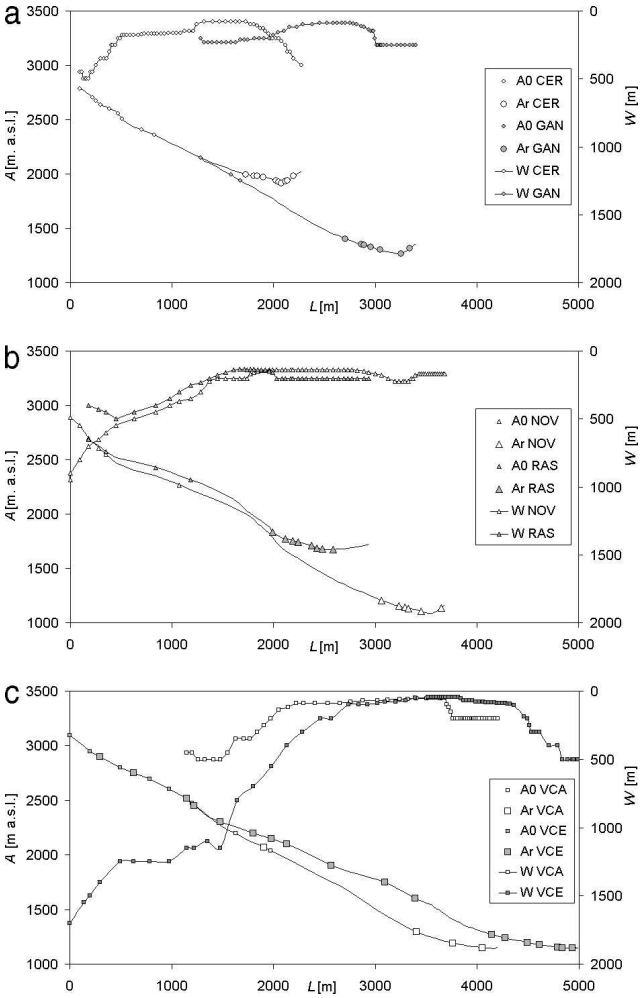

FIGURE 4. Observed avalanches tracks. On the left y axis with continuous line is shown the altitude profile [m a.s.l.]. A_0 indicates release or starting altitude of observed avalanche events. A_r indicates deposition or runout altitude of observed avalanche events. On the right y axis, with reverse (upside-down) coordinates it is shown the track width. (a) CER and GAN sites. (b) NOV and RAS sites. (c) VCA and VCE sites.

TABLE 4

Avalanche track geometry. E[s_0] is average track slope including the release area, E[s_f] is average track slope including the flow area, E[s_f] is average track slope including the runout area (average track slope). L_0' is percentage of track length including release area, L_f' is percentage of track length including flow area. For other abbreviations, see Table 1.

	CER	GAN	NOV	RAS	VCA	VCE	E[.]	CV[.]
E[s_0] (°)	30.2	30.3	30.0	30.1	29.2	28.3	29.7	2.6%
E[s_f] (°)	25.7	28.5	29.2	31.1	28.1	24.2	27.8	8.9%
E[s_r] (°)	20.9	23.2	25.6	29.7	24.9	21.5	24.3	13.2%
L_0' (%)	35%	30%	29%	39%	28%	30%	32%	13.1%
L_f' (%)	78%	73%	79%	80%	78%	78%	77%	3.1%

different altitude and track length), and therefore index value approach might be tentatively adopted.

PROBABILITY OF RELEASE

First, probability of avalanche release was investigated, as compared to snow depth at release. Preliminary analysis (reported in Bocchiola and Medagliani, 2007) showed that for 68% of the observed avalanches the triggering factor was linked to heavy precipitation in the 72 hours preceding the event (similar to e.g. Decaulne and Saemundsson, 2006). Therefore, it seems reasonable to investigate the probability of release as connected to the three day snowfall depth, H_{72d}. It is therefore assumed for simplicity that the release depth coincides with H_{72d} at the release site, $h_0 \approx H_{72d}$. Then, the regionally valid distribution of H_{72} evaluated by Bocchiola et al. (2006) was used to estimate the frequency of non-exceedance of h_0, $F_{h0,H72d}$. This was done by taking the dimensionless values of h_0, as $h_0^* = h_0/\mu_{H72}$, where μ_{H72} is the local average, or index value of H_{72}. This is possible because the variable h_0^* so obtained can be sketched as distributed according to a regionally valid distribution, as shown in Bocchiola et al. (2006). Then, the frequency of exceedance of the observed release depth h_0, F_{h0} has been evaluated using empirical plotting position. So doing, the ratio $F_0 = F_{h0,H72d}/F_{h0}$ gives an estimate of the probability that an avalanche occurs due to a given snowfall depth. The values of F_0 are reported in Figure 5. In spite of some sparseness, also due to possible uncertainty in the remote evaluation of snow depth at release, the observed distribution is well fit using a uniform distribution, UN. This is shown together with confidence limits for $\alpha = 5\%$, according to KS test. Notice from Table 1 that here no avalanche event was observed for $h_0 <$ 0.2 m. Therefore, if $H_{72} < 0.2$, the probability of an avalanche should be set to zero. The proposed distribution F_0 is reported in Table 2 and will be used here to trigger avalanche release conditioned on snowfall H_{72d} for simulation purposes.

RELEASE ALTITUDE

The observed avalanche altitude (i.e. altitude of snow fracture, or avalanche crown line) at release is variable, as shown in Figure 4. In each site, greatest (±) deviations are observed in the order of 10 to 15% or so with respect to the average value. The assumption is made here that while the average altitude at release is linked to local topography, a random component exists that results in changing of the release altitude for each single event. If one tentatively assumes that such a random component is similar in each avalanche site, a regional distribution of the dimensionless release altitude $A_0^* = A_0/\mu_{A0}$, with μ_{A0} average, or index local value, can be estimated by grouping the whole observed sample. The calculated sample frequency is shown in Figure 6. It can be seen that this has a relatively homogeneous behavior at the considered sites. The sample frequency is reasonably well accommodated using a Normal (henceforth NR) distribution, reported in Table 2.

AVALANCHE SHAPE AT RELEASE

Here, the shape of the avalanche release zone is investigated. The observed values of release width W_0 and length L_0 were adopted in the hypothesis of simplified avalanche geometry (i.e. release area featuring a rectangular shape with length L_0 and width W_0). Then, the statistical distribution of W_0 and L_0 was investigated. First, the existence of a dependence between h_0 and either W_0 or L_0 was investigated, because it might be that a link exists between the snow fracture depth and release area shape. However, no significant dependence was found between these

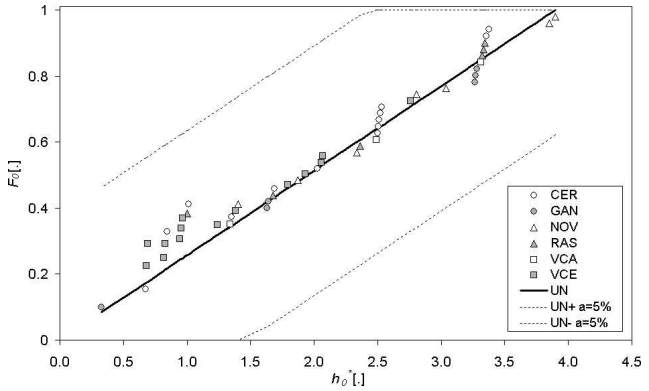

FIGURE 5. Release probability as a function of dimensionless release depth.

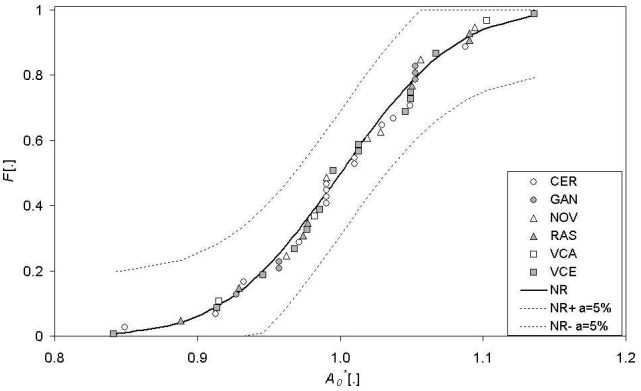

FIGURE 6. Frequency of the dimensionless avalanche release altitude.

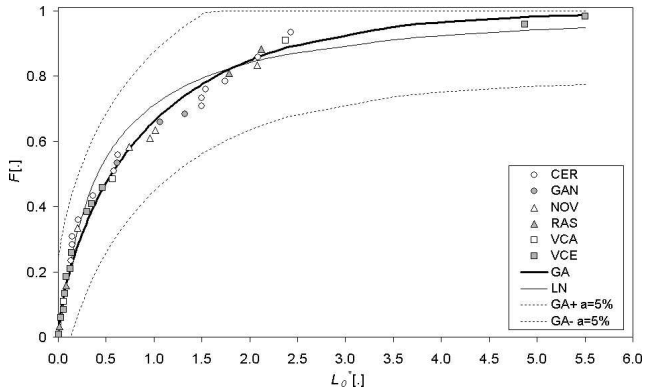

FIGURE 7. Frequency of the dimensionless avalanche release length.

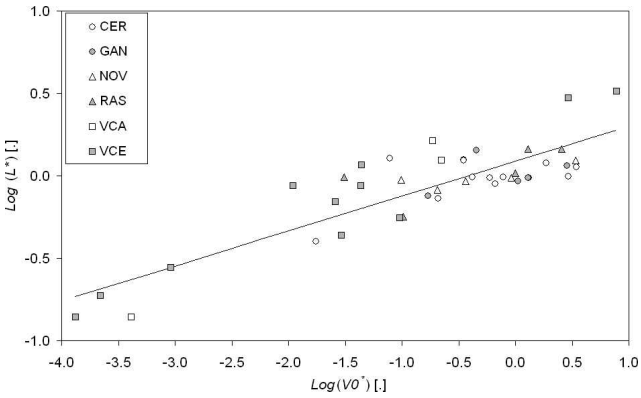

FIGURE 9. Dimensionless avalanche runout length *vs.* dimensionless volume at release.

variables, neither by visual assessment nor after correlation analysis (correlation coefficient on the whole sample $\rho_{W0,h0} = 0.13$ and $\rho_{L0,h0} = -0.09$, not significant at a reference $\alpha = 5\%$ confidence level). Therefore, avalanche width and length at release seem not linked to snow fracture depth, at least for these sites. Mutual dependence of L_0 and W_0 is also preliminarily investigated, showing in practice no significant correlation ($\rho_{L0,W0} = 0.16$, not significant for $\alpha = 5\%$). It is also made here the assumption that the average conditions at release are linked to local topography, while a random component exists, which is regionally valid. The sample frequency is then calculated of the dimensionless values, $W_0^* = W_0/\mu_{W0}$ and $L_0^* = L_0/\mu_{L0}$. These are reported in Figures 7 and 8. The frequencies of both W_0^* and L_0^* seem quite homogeneous in the considered sites and reasonably well accommodated by Gamma distributions (GA; the Lognormal distribution, LN, seems less fit), reported together with uncertainty bounds for confidence level $\alpha = 5\%$, according to the KS test. The parameters of the GA for W_0^* and L_0^* are reported in Table 2.

AVALANCHE RUNOUT VS. RELEASE VOLUME

Avalanche runout is linked to snow mass and volume (e.g. Hutter, 1996; Maggioni and Gruber, 2003) and avalanche dynamics models are sensitive to release mass (e.g. Voellmy, 1955; Bartelt et al., 1999), and greater avalanches run farther. However, dynamic models require proper parameter tuning, which is usually carried out for extreme (i.e. with high return periods, 30 to 300 or so in Switzerland; e.g. Salm et al., 1990) events, which are more likely to be mapped, while accurate information about more frequent (i.e. with low return periods) events is seldom available, thus making use of dynamic models less accurate. Further, dynamic model estimation and use for long-term simulation requires some probabilistic assessment of model parameters (e.g. Ancey et al., 2003; Naaim et al., 2004), which goes beyond the scope of the present paper. Here, the relation between snow mass at release and runout is directly investigated. In view of the different geometry and size of the considered avalanche sites, again dimensionless values are used with respect to the average, site specific, values, namely $V_0^* = V_0/\mu_{V0}$ and $L^* = L/\mu_L$. The hypothesis is made that a regionally homogeneous mechanism is present that relates avalanche volume and track length. This is similar to what is done in empirical methods based on topography (e.g. Lied and Bakkehøi, 1980; McClung et al., 1989; McClung and Mears, 1991), where regional analysis is used to increase sample dimensionality for model estimation (see e.g. Keylock, 2005). In Figure 9, it is shown how a linear regression fits well to the logarithms of the observed values of L^* against those of V_0^* for the considered sites. In Table 3 the calculated (power) law coefficients and their significance is reported. As expected, avalanches with greater volume tend to travel farther, while smaller ones have shorter track length. Albeit the explained variance is not very high ($R^2 = 0.74$), the proposed equation has the merit of providing a rapid evaluation of the expected runout distance of the avalanche. These proposed equations will be used for the assessment of avalanche runout here. Notice, however, that if a proper model parameterization is available, evaluation of the avalanche runout, depth, and velocity (i.e. pressure) can be obtained feeding the topographic and geometric properties of the avalanches to a dynamic model (e.g. Bocchiola et al., 2008b).

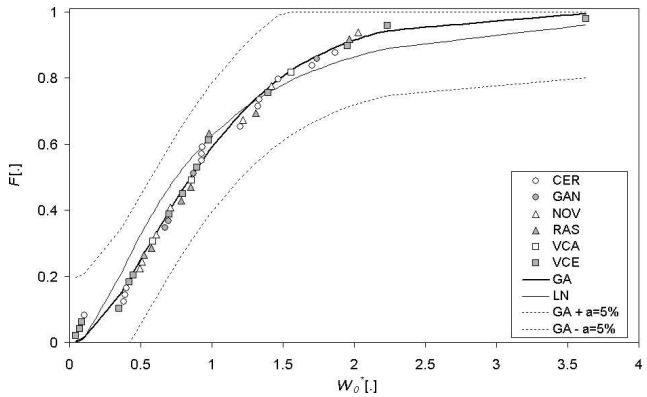

FIGURE 8. Frequency of the dimensionless avalanche release width.

AVALANCHE VOLUME AT RUNOUT

It is of interest to estimate the avalanche volume at runout, V_r. Usually, the latter is greater than the volume at release, V_0, due to snow entrainment (e.g. Sovilla and Bartelt, 2002; Sovilla et al., 2006, 2007). A growth index I_g can be estimated (e.g. Sovilla, 2004) giving the ratio between the snow mass at runout to that at release. This requires evaluation of both snow density and volume. Here, because no snow density measurements were taken in the post-event field survey, the simple hypothesis is adopted that snow density remains unchanged and the growth index is defined as $I_g = V_r/V_0$. I_g is here estimated for a number of 27 events showing acceptable evaluation of both V_r and V_0, according to the preliminary analysis reported above. The average observed value

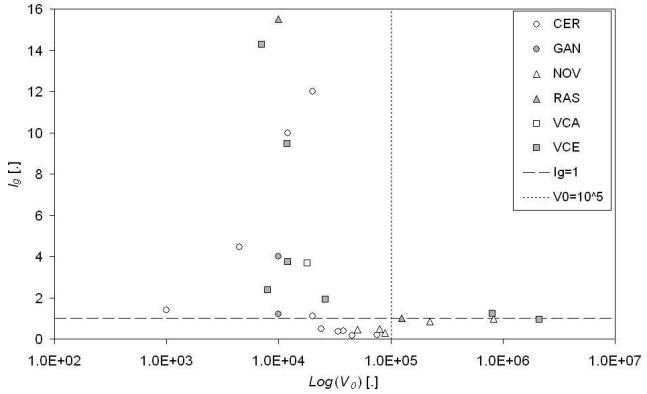

FIGURE 10. Estimated growth index, I_g, against release volume, V_0.

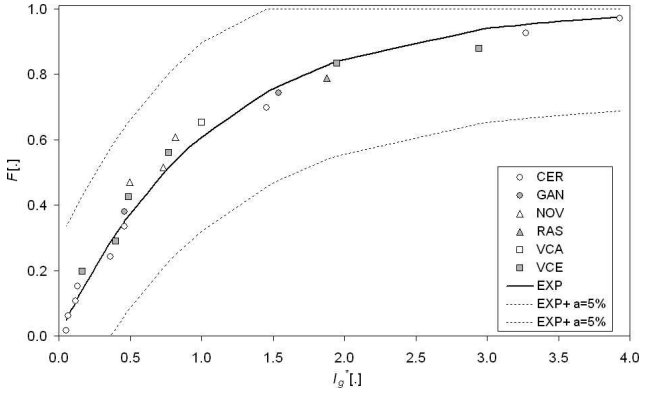

FIGURE 11. Frequency of the dimensionless growth index. $V_0 < 10^5$.

on the whole sample is of $E[I_g] = 3.5$, with a considerable variability, $CV[I_g] = 1.32$, ranging from the lowest value of 0.15 (CER15; see Table 1) to the greatest 15.5 (RAS7; see Table 1) (compare e.g. with Sovilla, 2004, giving an average value of $I_g = 4.6$ for a number of avalanches in Switzerland, with a considerable variability from about 1 to 12). Sovilla (2004) found a substantial independence between I_g and avalanche size and terrain characteristics along avalanche track. I_g is a complex function of snow depth and area at release, along-track erodible snow cover, and snow properties (e.g. Sovilla et al., 2006). Erodible snow cover is in turn linked to deposited snow cover before avalanche release, i.e. H_{72} along avalanche track and to snowline altitude (e.g. Bianchi Janetti and Gorni, 2007; Bianchi Janetti et al., 2008), and therefore depends on altitude (Bocchiola et al., 2006; Bocchiola and Rosso, 2007b). However, evaluation of eroded area and, therefore, snow mass is not straightforward and requires use of properly developed dynamic models (e.g. Sovilla et al., 2006; Bianchi Janetti et al., 2008).

Here, a number of cases (i.e. 8 cases; see Table 1) were found with $I_g \ll 1$, indicating along-track deposition. Apart from mistakes in volume evaluation that might still be present in spite of the preliminary assessment here carried out and explained in section 4.1, in some cases (i.e. CER7, CER12, CER15, NOV5), low values of I_g might be due to the occurrence of an avalanche in late spring (i.e. after mid April), when no considerable snow cover is available for along-track entrainment at low altitudes, and instead deposition might occur due to ground roughness. In other cases (i.e. CER13, CER14, NOV6, NOV9), avalanches occur during late autumn to winter (i.e. November to February), but still along-track deposition might occur.

A preliminary analysis showed that I_g is in practice uncorrelated to snow depth, avalanche width, and length at release, as well as to avalanche runout length. Plotting of I_g against release volume V_0 is reported in Figure 10. This can be roughly split into two parts. For low values of V_0 (i.e. $V_0 < 10^5$ or so), I_g ranges from about 1 to more than 15, with no apparent link to V_0. For $V_0 > 10^5$ or so, in practice $I_g = 1$. The five avalanche events when $V_0 > 10^5$ occurred in early to late spring (see Table 1; NOV4, NOV8, VCE10, VCE11, and RAS8 [the date of RAS8 is not known exactly, but it happened in late spring]), when little snow cover was available at low altitudes, thus resulting in little snow uptake, if any. Here, it is assumed for simplicity that for $V_0 < 10^5$, I_g is in practice a random variable, in view of its clear independence from V_0, while for $V_0 \geq 10^5$, $I_g = 1$. Albeit this approach is very simple in respect to the complexity entailed in understanding and modeling avalanche mass uptake, it seems that it might be used to capture the statistical properties of the phenomenon and to evaluate in a first approximation the statistics of avalanche volumes at deposition. It was observed here that for $V_0 < 10^5$, the dimensionless growth index $I_g^* = I_g/\mu_{Ig}$, with μ_{Ig} average local value, can be fairly well accommodated according to an exponential (EXP) statistical distribution, as shown in Figure 11. Therein, it is seen that a pretty homogeneous distribution is obtained by grouping the single site values of I_g^*. This indicates that a regionally similar random component seems to exist that results in variability of the growth index for each event. Therefore, we introduce here random value of I_g^* as from the proposed EXP distribution, reported in Table 3.

Long-term Simulation of Avalanche Series

SIMULATION STRATEGY AND APPLICATION TO VALLECETTA AVALANCHE SITE

Avalanche dynamics simulation is carried out daily. First, to simulate snowfall depth at the release altitude in the Vallecetta site, the average value of H_d needs to be scaled for the release altitude A_0, as from the proposed equation in Table 3.

For the Vallecetta site, use the average value of the release altitude, $E[A_0] = 2697$ results in $\mu_{Hd} = 12.1$ cm. Using this value, every day the increase in snowpack depth H_d is simulated according to the model proposed in the section *Methods: Snow Depth Data* and a simulated series of H_{72d} is obtained. Based on H_{72d}, the probability p_{av} that an avalanche occurs is evaluated using the UN distribution in Figure 5. Extraction of a random value from a UN distribution is used to evaluate occurrence of an avalanche according to a binomial distribution (yes/no with parameter p_{av}). If an avalanche occurs at day d, its release depth is set to $h_0 = H_{72d}$. No snow drift load is applied in the avalanche release area, as suggested by the *Sp*. Analysis of the avalanche database, including qualitative meteorological information, indicated presence of strong wind in the 3 days before the event only on one date (1 November 1986) out of 21. So, one may assume here that wind upload is not preponderant for avalanche release. Further, neither estimation of wind snow load is available here, nor do we know of any accurate formula for its estimation for this area. However, because we estimate release probability using observed snow depth at release, which may include wind load, we in some way account for such phenomena. Notice that in those cases where snow load can be estimated, it can be used in the procedure. In case of an avalanche at day d, evaluation of H_{72} in the next day $d + 1$, H_{72d+1} accounts for avalanche occurrence (i.e.

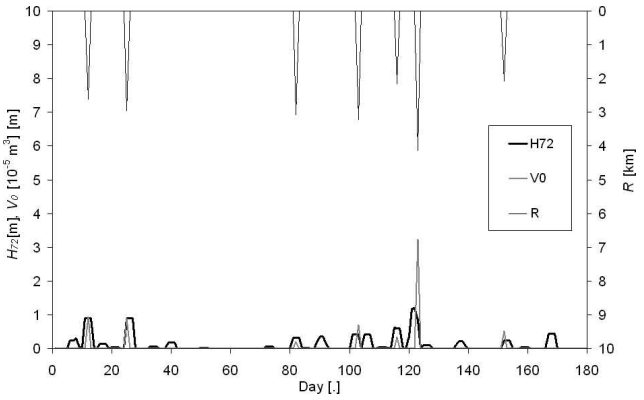

FIGURE 12. Long-term avalanche simulation, Vallecetta mountain. On the left *y* axis are shown the simulated values of H_{72d}, and volume at release V_0 for avalanche events in a sample year. On the right *y* axis, with reverse (upside-down) coordinates is shown the corresponding runout from the start of the avalanche track, *R*.

in practice, $H_{72d+1} = H_{d+1}$). The second step is the random simulation of the release (crown) altitude A_0^*, according to the NR distribution proposed in the section *Release Altitude*, and $A_0 = \mu_{A0} \cdot A_0^*$, with the further constraint that A_0 is included into the release zone as deduced in the section *Avalanche Track Geometry*. Then, dimensionless release width and depth W_0^*, L_0^* are randomly extracted from the Gamma distributions reported in Table 3, and $W_0 = \mu_{W0} \cdot W_0^*$, $L_0 = \mu_{L0} \cdot L_0^*$, with the boundary conditions given by topography (i.e. greatest width and length). Avalanche release volume is then estimated as $V_0 = h_0' \cdot L_0 \cdot W_0$, where h_0' is the release depth as corrected for local slope following the *Sp* procedure (e.g. Salm et al., 1990). Then, dimensionless runout L^* can be evaluated as a function of dimensionless release volume V_0^* as explained in the section *Avalanche Runout vs. Release Volume*, and $L = L^* \cdot \mu_L$. Then, runout volume V_r is evaluated according to V_0. If $V_0 < 10^5$, I_g^* is extracted from the EXP distribution reported in the section *Avalanche Volume at Runout*, and $V_r = V_0 \cdot \mu_{Ig} \cdot I_g$. If $V_0 \geq 10^5$, $V_r = V_0$. A sample year of simulation is reported in Figure 12. The sequence of H_{72d} is reported, together with information of avalanche occurrence, volume at release V_0, and runout. We report here the absolute runout position measured from the start of the avalanche track, *R*, rather than the track length, *L*, which is instead relative to the starting point, which changes from case to case. In this particular year, seven avalanche events were synthetically simulated. Here, simulation was carried out for a number of years $n_{tot} = 195$, consistent with the snowfall simulation in the section *Methods: Snow Depth Data*. Again, to decrease sample effects, a number of 100 simulations were carried out, for a total of $1.95 \cdot 10^4$ years.

RESULTS

In Table 5, some explanatory statistics are reported concerning the avalanche release volume, V_0, absolute runout, *R*, and deposition volume, V_r. The full sample average is reported (including the whole set of simulated avalanches, e.g. E[V_0]), together with the sample average of the extreme avalanches (i.e. the greatest annual values E[V_{0max}]) and the greatest observed value, of interest for land use planning (e.g. MAX[V_0]). These are compared with the same statistics as obtained from the available sample of data. Notice that in view of the relatively small sample size, the confidence limits $\sigma \pm$ for the average values are considerably wide. Also, notice that for the full sample, average comparison against the observed values is particularly difficult,

TABLE 5

Vallecetta mountain. Some observed and simulated statistics of avalanche data. Symbol $\sigma \pm$ indicates sigma bounds (i.e. mean $\pm$ standard deviation). Notice the relative width of the sigma bounds, in view of the small sample size. Bold indicates values falling outside the sigma bounds.

Var	N_{obs}	Obs.	$\sigma \pm$	Sim.
E[V_0] (m^3)	11	2.31E^5	3.30E^4–4.29E^5	0.95E^5
E[V_{0max}] (m^3)	6	3.59E^5	7.00E^3–7.11E^5	2.18E^5
MAX[V_0] [m^3]	—	2.00E^6	—	1.96E^6
E[V_r] (m^3)	13	2.89E^5	1.27E^5–4.51E^5	1.76E^5
E[V_{rmax}] (m^3)	7	3.76E^5	1.01E^5–6.51E^5	3.77E^5
MAX[V_r] (m^3)	—	2.12E^6	—	2.37E^6
E[*R*] (m)	21	2797	2500–3000	**2430**
E[R_{max}] (m)	16	3161	2840–3490	2976
Max[*R*] (m)	—	4930	—	5041

because the observed statistics are considerably skewed towards the greatest values (i.e. those more likely to be observed), thus resulting in likely overestimation. In view of the small available sample, higher order statistics (e.g. coefficient of variation) were not considered for the comparison.

Also considering the relevant degree of uncertainty of the proposed statistics, one notices that the proposed model for long-term simulation results in estimated avalanche features that are compatible with those observed at the investigated sites.

Average yearly number of avalanches was $n_{av} = 3.1$. Comparison with the observed database is probably senseless, because several (minor) avalanches are likely to be neglected. As a rough comparison, Naaim et al. (2004), referring to a ''well known avalanche path'' reported of a number of observed avalanches of about 153 in 72 years. On average, here no avalanche occurrence was found in 4.2% of the years (i.e. the average number of years with no avalanche is $n_0 = 8.2$ out of 195), giving the probability that in a given year no avalanche is observed at the Vallecetta site. In Figures 13 to 15 there are reported the synthetically obtained plotting positions of the greatest annual values of the runout, release, and deposition volume, R_{max}^*, V_{0max}^*, V_{rmax}^*, made dimensionless with respect to their average values in Table 5. These are compared with the dimensionless sample values from the six investigated sites, used to increase sample dimensionality and to allow more likely estimation of the frequency of occurrence for the considered events. To clarify this issue, one could consider e.g. the VCE11 event ($R_{max} = 4930$, $R_{max}^* = 1.56$), which occurred in 1886. According to the empirical plotting position from the single site analysis (i.e. using the available local data, for a number of 15 years) its estimated return period (using APL plotting position, see the section *Distribution of* H_{72}) would be $T_{VCE11,site} = 23$ years. One can attain unbiased estimation of the related return period according to the historical flood (here, avalanches) approach, giving $T_{hist} = (n + 1)/(n' + 1)$, with *n* years of observation and n' number of years when a given value is exceeded (e.g. Kottegoda and Rosso, 1997; Bocchiola et al., 2003). Here, $R_{maxVCE11}^*$ was attained once over the last 123 (from 1886 to 2007) years, therefore giving $T_{VCE11,hist} = 124/2 = 62$ years, with sigma bounds (see Bocchiola et al., 2003, Equation 11) $T_{VCE11,hist} \pm$ = 35–198 years. Using the regional plotting position of the dimensionless observed runout values, one obtains $T_{VCE11,reg} = 75$ years (i.e. $y_T = 4.32$; see Fig. 14), closer to the unbiased value as reported than the return period for single site plotting position. The synthetically obtained plotting position of V_{0max}^* (Fig. 13) seems to fit well the observed one. Some discordancy is observed for $T < 2$ years or so. However, this could be due to improper

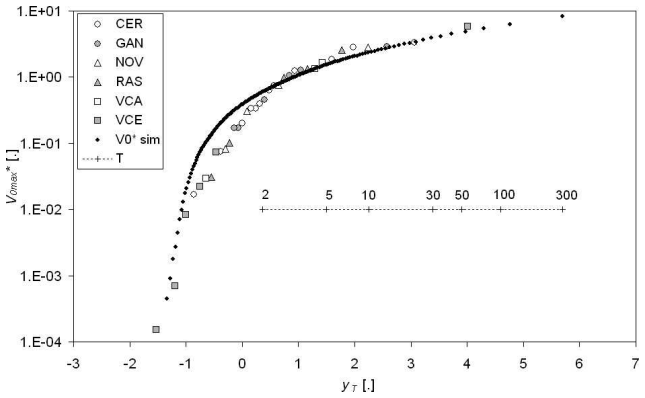

FIGURE 13. Long-term avalanche simulation, Vallecetta mountain. Dimensionless greatest annual release volume V_{0max}^*. Observed plotting position from the dimensionless sample of the six avalanche sites.

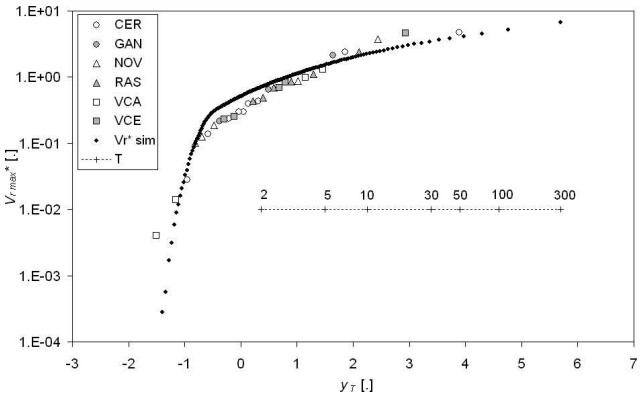

FIGURE 15. Long-term avalanche simulation, Vallecetta mountain. Dimensionless greatest annual runout volume V_{rmax}^*. Observed plotting position from the dimensionless sample of the six avalanche sites.

labeling of small avalanches as greatest annual ones, in turn possibly resulting from either lack of observation of small avalanche phenomena, or poor assessment of the release volumes for such small avalanches, as reported. Runout R_{max}^* in Figure 14 seems quite well represented for the whole range of considered return periods. Eventually, the deposition volumes (Fig. 15) seem well estimated, with a slight discordance for $T < 2$ or so, again possibly related to poor assessment of small avalanches properties.

DISCUSSION

The acceptable fitting of the simulated avalanche properties to the observed values as reported seems to indirectly confirm the capacity of the proposed model to reasonably represent an avalanche regime in a given site. In spite of the small sample size, suggesting care in interpretation of the results, the proposed approach seems valuable for its application in the field of geomorphology and ecology of mountain ranges, where snow avalanche magnitude, runout, and frequency are acknowledged to play a predominant role.

The present model provides a description of long-term avalanche occurrence, to be used as an input for geomorphologic theories. If a simple, data-driven parameterization would be introduced to link, say avalanche properties with erosional features (as in e.g. Bell et al., 1990), the present approach would provide an estimation of these properties also for low frequency of occurrence, thus allowing long-term evaluation of morphological effects of snow mass movement.

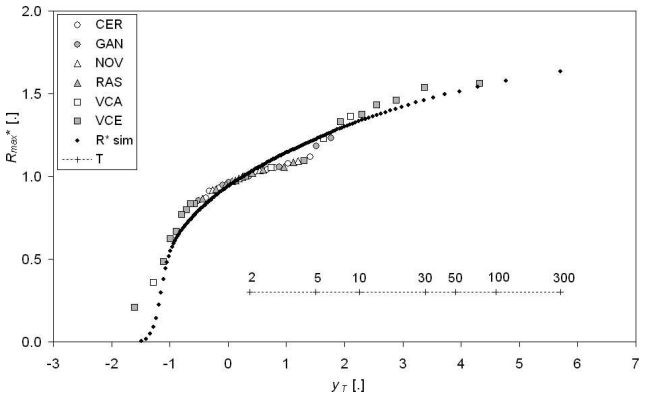

FIGURE 14. Long-term avalanche simulation, Vallecetta mountain. Dimensionless greatest annual release runout R_{max}^*. Observed plotting position from the dimensionless sample of the six avalanche sites.

The present approach does not explicitly include use of a snow dynamics model, the parameterization of which goes somewhat beyond the scope of the present paper, while runout and snow uptake are more simply assessed.

However, in case a dynamics model would be available, including i.e. sediment transport from snow avalanches, or vegetation removal (as e.g. in Bartelt and Stöckly, 2001), still the input given by the model would be valuable for long-term simulation. Because H_{72} can be used as a condition for erodible snow cover for mass uptake simulation (Bianchi Janetti and Gorni, 2007; Bianchi Janetti et al., 2008), the proposed model may give valuable input for long-term avalanche dynamics including mass uptake (e.g. Naaim et al., 2003; Eglit and Demidov, 2005; Barbolini et al., 2005; Sovilla et al., 2006, 2007). Furthermore, the present approach may be modified to include an assessment of medium to long-term scenarios of changes in snowfall dynamics on the avalanche frequencies. Because changes in avalanche regime affect Alpine ecosystems in many ways (e.g. Erschbamer, 1989; Mace et al., 1996; Krajick, 1998; Kulakowski et al., 2006), long-term avalanche scenarios are of interest.

The proposed model accounts for snowfall-triggered avalanche events, usually resulting in dry, or moderately wet flowing avalanches. Albeit these seem to cover the vast majority of the observed avalanche events here (see also e.g. Decaulne and Saemundsson, 2006), and are in widespread use in practice to model avalanche occurrence for long-term simulation, model tuning, and hazard evaluation (Salm et al., 1990; Burkard and Salm, 1992; Bartelt et al., 1999; Ancey et al., 2004; Barbolini et al., 2004), different triggering mechanisms can be observed. These include more frequent wet avalanches, or less frequent ($T \approx 40$ years or so) slush avalanches, including mud flows, both usually occurring at spring thaw (May to June, see e.g. Jomelli and Bertran, 2001). Note that the approach here shown accounts in practice for both dry and wet avalanches, without an explicit distinction. This may be introduced e.g. by considering snowpack state modeling in time (e.g. for snow depth and density), to be included in the model. As reported, for the considered avalanches no measurements of snow density were available, which is also of interest to evaluate avalanche type (e.g. Freppaz et al., 2006). For the considered area, the density of freshly fallen

snow, H_n, is in practice a LN distributed random variable, with mean slightly decreasing with altitude (e.g. Bocchiola and Rosso, 2007a; Medagliani et al., 2007). Its observed average is $\rho_{n,av}$ = 123 kg m^{-3} (and $\rho_{n,\mathrm{BOR}}$ = 103 kg m^{-3}; Bocchiola and Rosso, 2007a). The density ρ_s of the snowpack H_s notably changes with the season (i.e. with day in the winter season d; see e.g. Elder et al., 1991). For instance, Martinelli et al. (2004) used data from a number of 196 snow pits in the Lombardia region, mainly concentrated in the BOR area and ranging from November to May for the period 1997–2002, and found ρ_s = 161–618 kg m^{-3}, depending linearly on d and averaging to $\rho_{s,av}$ = 324 kg m^{-3}. Notice that the *Sp* suggests use of ρ_s = 300 kg m^{-3} for avalanche pressure calculation (Salm et al., 1990; Barbolini et al., 2004), thus considering in practice moderately wet avalanches. Because here the daily variation of H_s, i.e. H_d, is used according to the *Sp*, use of ρ_s might be suggested. Also, one could explicitly evaluate snow settling during the three days before the avalanche events to calculate the density of H_{72} (as e.g. in Martinec and Rango, 1991). Here, the reasonable matching of the statistics of the simulated values of H_{72d} with those observed in the BOR snow series seems to indicate that no considerable settling effect needs to be accounted for when using snowpack series for H_{72} simulation.

Notice further that the proposed snowfall simulation model with slight changes is suitable for more complex approaches. For instance, it could be used to provide an input for simulation of snowpack dynamics using a more refined model (e.g. SNOWPACK; Bartelt and Lehning, 2002), say by including long-term simulation of fresh snow depth and density based on suitable distributions (e.g. Bocchiola and Rosso, 2007a).

Conclusions

Here, a relatively simple framework based on regional analysis is drawn that allows the building of statistically consistent series of daily avalanche occurrence and magnitude in a given site. Because the proposed approach combines statistical interpretation of climatic forcing with regional analysis of observed avalanche tracks, more accurate description is achieved of the avalanche occurrence process with respect to the presently adopted methods solely based either on runout analysis of extreme (i.e. with high return periods) events, or on derivation of extreme avalanches from extreme snowfalls. In turn, more comprehensive data are required, including avalanche volumes and geometry, as well as snowfall records. However, provided a reasonable regional homogeneity and topographic similarity holds, data from avalanches occurring at different sites inside a given region can be used to increase sample dimensionality. Further improvement could include explicit evaluation of different types of avalanches, and the introduction of different snow density, according to the available literature and the season. Also, further developments will include strategies for the evaluation of the index values of the observed avalanche features starting from some *a priori* measurable indexes, including e.g. local topography. This would allow use of the proposed approach also in those places where no avalanche data are available to evaluate the required index values. Coupling with an avalanche dynamics model could provide a more physically based description of long-term avalanche dynamics for avalanche hazard assessment. In the future, we will try to extend the study area, so hopefully increasing the avalanche database, to reduce uncertainty in our findings.

Acknowledgments

The authors kindly acknowledge Eng. Alice Pagani and Eng. Giovanni Sala for their contribution to the present research, developed during their MS thesis. The authors kindly acknowledge the personnel of AINEVA, in Bormio, and the Rangers of Sondrio City (Corpo Forestale dello Stato) for providing the snow and avalanche data from their archives and for helpful suggestions. ARPA Lombardia is acknowledged for providing snow data. Funding for the research presented in the present paper was granted by the European Community, through the EU projects AWARE (EC contract 012257) and IRASMOS (EC Contract 018412) and by the CARIPLO foundation of Italy through the project CARIPANDA.

References Cited

Ackroyd, P., 1987: Erosion by snow avalanche and implications for geomorphic stability, Torlesse Range, New Zealand. *Arctic, Antarctic, and Alpine Research*, 19(1): 65–70.

Ancey, C., Meunier, M., and Richard, D., 2003: Inverse problem in avalanche dynamics models. *Water Resources Research*, 39(4): 1099, doi: 10.1029/2002WR001749.

Ancey, C., Gervasoni, C., and Meunier, M., 2004: Computing extreme avalanches. *Cold Regions Science and Technology*, 39: 161–180.

Arena Lo Riggio, E., Mura, M., Bocchiola, D., Rulli, M. C., and Rosso, R., 2009: Un modello a formulazione energetica per il calcolo dinamico delle valanghe [An energy formulation based model for dynamic calculation of avalanche]. *Neve e Valanghe*, 65: 32–41 (in Italian, with abstract in English).

Bacchi, B., Becciu, G., and Kottegoda, N., 1994: Bivariate exponential model applied to intensities and durations of extreme rainfall. *Journal of Hydrology*, 155(1–2): 225–236.

Baeriswyl, P. A., and Rebetez, M., 1997: Regionalization of precipitation in Switzerland by means of principal components analysis. *Theoretical and Applied Climatology*, 58: 31–41.

Barbolini, M., Gruber, U., Keylock, C. J., Naaim, M., and Savi, F., 2000: Application of statistical and hydraulic-continuum dense-snow avalanche models to five real European sites. *Cold Regions Science and Technology*, 31: 133–149.

Barbolini, M., Natale, L., and Savi, F., 2002: Effect of release conditions uncertainty on avalanche hazard mapping. *Natural Hazards*, 25: 225–244.

Barbolini, M., Cappabianca, F., and Savi, F., 2003: A new method for estimation of avalanche distance exceeded probability. *Surveys in Geophysics*, 24: 587–601.

Barbolini, M., Natale, L., Cordola, M., and Tecilla, G., 2004: Guidelines for mapping of avalanche hazard prone areas [Linee Guida metodologiche per la perimetrazione delle aree esposte al pericolo di valanghe]. *Neve e Valanghe*, 53: 6–13 (in Italian with abstract in English).

Barbolini, M., Biancardi, A., Cappabianca, F., Natale, L., and Gagliardi, M., 2005: Laboratory study of erosion processes in snow avalanches. *Cold Regions Science and Technology*, 43: 1–9.

Bartelt, P., and Lehning, M., 2002: A physical SNOWPACK model for the Swiss avalanche warning. Part I: numerical model. *Cold Regions Science and Technology*, 35: 123–145.

Bartelt, P., and Stöckly, V., 2001: The influence of tree and branch fracture, overturning and debris entrainment on snow avalanche flow. *Annals of Glaciology*, 32: 209–216.

Bartelt, P., Salm, B., and Gruber, U., 1999: Calculating dense-snow avalanche runout using a Voellmy-fluid model with active/passive longitudinal straining. *Journal of Glaciology*, 45: 242–254.

Bebi, P., Kienast, F., and Schonenberger, W., 2001: Assessing structures in mountain forests as a basis for investigating the forests' dynamics and protective function. *Forest Ecology and Management*, 145: 3–14.

Bell, L., Gardner, J., and De Scally, F., 1990: An estimate of snow avalanche debris transport, Kaghan Valley, Himalaya, Pakistan. *Arctic, Antarctic, and Alpine Research*, 22(3): 317–321.

Benda, L. E., and Sias, J. C., 2003: A quantitative framework for evaluating the mass balance of in stream organic debris. *Forest Ecology and Management*, 172: 1–16.

Bianchi Janetti, E., and Gorni, E., 2007: Avalanche dynamics calculations: a study on snow cover height in Switzerland with regional approach. Master thesis. Politecnico di Milano, Italy (available at: http://www.diiar.polimi.it/cimi/persona.asp?id=35).

Bianchi Janetti, E., Gorni, E., Sovilla, B., and Bocchiola, D., 2008: Regional snow depth estimates for avalanche calculations using a 2D model with snow entrainment. *Annals of Glaciology*, 49: 63–70.

Blikra, L. H., and Sæmundson, T., 1998: The potential of sedimentology and stratigraphy in avalanche-hazard research. *I: NGI Publication*, 203: 60–64 (ISSN: 0078-1193).

Bocchiola, D., and Medagliani, M., 2007: Morphology of avalanches: a study in the Bormio area [Morfologia delle valanghe, uno studio nell'area del Bormiese]. *Neve e Valanghe*, 3: 70–79 (in Italian with abstract in English) (available upon request or at: http://www.aineva.it/presenta.html).

Bocchiola, D., and Rosso, R., 2007a: The distribution of daily Snow Water Equivalent in the central Italian Alps. *Advances in Water Resources*, 30: 135–147.

Bocchiola, D., and Rosso, R., 2007b: The use of regional approach for hazard mapping at an avalanche site in northern Italy. *Advances in Geosciences*, 14: 1–9.

Bocchiola, D., De Michele, C., and Rosso, R., 2003: Review of recent advances in index flood estimation. *Hydrology and Earth System Sciences*, 7(3): 283–296.

Bocchiola, D., Medagliani, M., and Rosso, R., 2006: Regional snow depth frequency curves for avalanche hazard mapping in central Italian Alps. *Cold Regions Science and Technology*, 46(3): 204–221.

Bocchiola, D., Bianchi Janetti, E., Gorni, E., Marty, C., and Sovilla, B., 2008a: Regional evaluation of three day snow depth frequency curves for Switzerland. *Natural Hazard and Earth System Sciences*, 8: 685–705.

Bocchiola, D., Bianchi Janetti, E., and Medagliani, M., 2008b: A regional approach for the simulation of extreme snow avalanches: a case study in the Italian Alps. Oral presentation and abstract at EGU General Assembly, Vienna, 13–18 April 2008.

Bovis, M. J., and Mears, A. I., 1976: Statistical prediction of snow avalanche runout from terrain variables in Colorado. *Arctic and Alpine Research*, 8(1): 115–120.

Bozhinskiy, A. N., and Chernous, P. A., 1986: Probability model of snow stability on mountain slopes. Materialy Glyatsiologicheskikh Issledovanii. *Khronika, Obsuzhdeniya*, 55: 53–60 (available in English in Kotlyakov, V. M. [ed.], 1997: 34 Selected papers on main ideas of the soviet glaciology 1940s–1980s. Moscow: Glaciological Association of Russia, 411–420).

Bozhinskiy, A. N., and Losev, K. S., 1998: *The Fundamentals of Avalanche Science*. SLF Davos, Mitteilungen n. 55, 280 pp.

Burkard, A., and Salm, B., 1992: Die bestimmung der mittleren anrissmachtigkeit d_0 zur berechnung von fliesslawinen [Estimate of the average release depth d_0 for the calculation of flowing avalanches]. Davos: Internal Report of the Swiss Federal Institute for Snow and Avalanche Research, No. 668 (in German; also available in French under the title: Estimation de l'epaisseur moyenne de declenchement d_0 pour le calcul des avalanches coulantes, translated into French by C. Ancey, Cemagref, 1994).

Casteller, A., Stöckli, V., Villalba, R., and Mayer, A. C., 2007: An evaluation of dendro-ecological indicators of snow avalanches in the Swiss Alps. *Arctic, Antarctic, and Alpine Research*, 39(2): 218–228.

Christen, M., Bartelt, P., and Gruber, U., 2002: *AVAL-1D: Numerical Calculations of Dense Flow and Powder Snow Avalanches, User Manual* Eidgenössische Institut für Schnee und Lawinenforschung, SLF Davos: Switzerland,

Cowpertwait, P. S. P., 1994: A generalized point process model of rainfall. *Proceedings of the Royal Society of London*, A447: 23–37.

Cowpertwait, P. S. P., 1995: A generalized spatial-temporal model of rainfall based on a cluster point process. *Proceedings of the Royal Society of London*, A450: 163–175.

De Michele, C., and Rosso, R., 2001: Uncertainty assessment of regionalized flood frequency estimates. *Journal of Hydrological Engineering*, 6(6): 453–459.

De Michele, C., and Rosso, R., 2002: A multi-level approach to flood frequency regionalization. *Hydrology and Earth System Sciences*, 6(2): 185–194.

De Scally, F. A., and Owens, I. F., 2005: Depositional processes and particle characteristics on fans in the Southern Alps, New Zealand. *Geomorphology*, 69: 46–56.

Decaulne, A., and Saemundsson, T., 2006: Geomorphic evidence for present-day snow-avalanche and debris-flow impact in the Icelandic Westfjords. *Geomorphology*, 80: 80–93.

Eglit, M. E., and Demidov, K. S., 2005: Mathematical modeling of snow entrainment in avalanche motion. *Cold Regions Science and Technology*, 43: 10–23.

Elder, K., Dozier, J., and Michaelsen, J., 1991: Snow accumulation and distribution in an alpine watershed. *Water Resources Research*, 27(7): 1541–1552.

Elder, K., Rosenthal, W., and Davis, R. E., 1998: Estimating the spatial distribution of snow water equivalence in a montane watershed. *Hydrological Processes*, 12: 1793–1808.

Erschbamer, B., 1989: Vegetation on avalanche paths in the Alps. *Vegetatio*, 80: 139–146.

Fetherston, K. L., Naiman, R. J., and Bilby, R. E., 1995: Large woody debris, physical process and riparian forest development in montane river networks of the Pacific Northwest. *Geomorphology*, 13: 133–144.

Freppaz, M., Lunardi, S., Maggioni, M., Valfrè di Bonzo, F., and Bizzocchi, T., 2006: Valanghe ed erosione del suolo: risultati preliminari ottenuti in due siti sperimentali in Valle D'Aosta [Soil erosion of avalanches: preliminary results from two sites in Aosta Valley]. *Neve e Valanghe*, 59: 34–41 (in Italian with abstract in English) (available upon request or at: http://www.aineva.it/pubblica/neve59/4_erosione.html).

Fuchs, S., and McAlpin, M. C., 2005: The net benefit of public expenditures on avalanche defence structures in the municipality of Davos, Switzerland. *Natural Hazards and Earth Systems Science*, 5: 319–330.

Fuchs, S., Bründl, M., and Stötter, J., 2004: Development of avalanche risk between 1950 and 2000 in the Municipality of Davos, Switzerland. *Natural Hazards and Earth Systems Science*, 4: 263–275.

Gabriele, S., and Arnell, N., 1991: A hierarchic approach to regional flood frequency analysis. *Water Resources Research*, 27(6): 1281–1289.

Gardner, J. S., 1983: Observations on erosion by wet snow avalanches, Mount Rae area, Alberta, Canada. *Arctic and Alpine Research*, 15(2): 271–274.

Geertsema, M., and Pojar, J. J., 2007: Influence of landslides on biophysical diversity—A perspective from British Columbia. *Geomorphology*, 89: 55–69.

Gruber, U., and Sardemann, S., 2003: High-frequency avalanches: release area characteristics and run-out distances. *Cold Regions Science and Technology*, 37: 439–451.

Heckmann, T., Wichmann, V., and Becht, M., 2002: Quantifying sediment transport by avalanches in the Bavarian Alps—First results. *Zeitschrift für Geomorphologie*, N.F., Suppl.-Bd. 127: 137–152.

Heckmann, T., Wichmann, V., and Becht, M., 2005: Sediment transport by avalanches in the Bavarian Alps revisited—A perspective on modelling. *Zeitschrift für Geomorphologie*, N.F. Suppl. 138: 11–25.

Hopf, J., 1998: An overview of natural hazard zoning with special reference to avalanches. *In* Proceedings of the Anniversary Conference for the 25 Years of Snow Avalanche Research at NGI, Voss, Norway, 12–16 May 1998. Norwegian Geotechnical Institute Publications No. 203, 28–35.

Hutter, K., 1996: Chapter 11: avalanche dynamics. *In* Singh, V. (ed.), *The Hydrology of Disasters*. Dordrecht: Kluwer Academic Publishers, 319–390.

Jomelli, V., and Bertran, P., 2001: Wet snow avalanche deposits in the French Alps: structure and sedimentology. *Geografiska Annaler*, 83A: 15–28.

Jomelli, V., and Francou, B., 2000: Comparing the characteristics of rockfall talus and snow avalanche landforms in an Alpine environment using a new methodological approach: Massif des Ecrins, French Alps. *Geomorphology*, 35: 181–192.

Katz, R. W., 1999: Extreme value theory for precipitation: sensitivity analysis for climate change. *Advances in Water Resources*, 23: 133–139.

Katz, R. W., Parlange, M. B., and Naveau, P., 2002: Statistics of extremes in hydrology. *Advances in Water Resources*, 25: 1287–1304.

Keylock, C. J., 2005: An alternative form for the statistical distribution of extreme avalanche runout distances. *Cold Regions Science and Technology*, 42: 185–193.

Keylock, C. J., and Barbolini, M., 2001: Snow avalanche impact pressure—Vulnerability relations for use in risk assessment. *Canadian Geotechnical Journal*, 38: 227–238.

King, R. H., and Brewster, G. R., 1978: The impact of environmental stress on subalpine pedogenesis, Banff National Park, Alberta. *Arctic and Alpine Research*, 10(2): 295–312.

Kottegoda, N., and Rosso, R., 1997: *Statistics, Probability and Reliability for Civil and Environmental Engineers*. New York: McGraw-Hill.

Kottegoda, N. T., Natale, L., and Reiteri, E., 2000: Statistical modelling of daily streamflows using rainfall input and curve number technique. *Journal of Hydrology*, 234: 170–186.

Krajick, K., 1998: Ecology—Animals thrive in an avalanche's wake. *Science*, 279: 1853.

Kuhn, M., 2003: Redistribution of snow and glacier mass balance from a hydro meteorological model. *Journal of Hydrology*, 282: 95–103.

Kulakowski, D., Rixen, C., and Bebi, P., 2006: Changes in forest structure and in the relative importance of climatic stress as a result of suppression of avalanche disturbances. *Forest Ecology and Management*, 223: 66–74.

Lied, K., and Bakkehøi, S., 1980: Empirical calculations of snow avalanche run-out distance based on topographic parameters. *Journal of Glaciology*, 26(94): 165–177.

Luckman, B. H., 1977: The geomorphic activity of snow avalanches. *Geografiska Annaler*, 59: 31–48.

Mace, R. D., Waller, J. S., Manley, T. L., Lyon, L. J., and Zuuring, H., 1996: Relationships among grizzly bears, roads and habitat in the Swan Mountains, Montana. *Journal of Applied Ecology*, 33: 1395–1404.

Maggioni, M., and Gruber, U., 2003: The influence of topographic parameters on avalanche release dimension and frequency. *Cold Regions Science and Technology*, 37(3): 407–419.

Martinec, J., and Rango, A., 1991: An indirect evaluation of snow reserves in mountain basins. *In* Bergmann, H., Lang, H., Frey, W., Issler, D., and Salm, B. (eds.), *Proceedings: Snow, Hydrology and Forest in High Alpine Areas*. Vienna: IAHS Publication 205, 111–120.

Martinelli, M., 1986: A test of the avalanche runout equations developed by the Norwegian Geotechnical Institute. *Cold Regions Science and Technology*, 13: 19–33.

Martinelli, O., Modena, D., Bocchiola, D., De Michele, C., and Rosso, R., 2004: La risorsa idrica nivale in Lombardia [The snow water resources in Lombardia region]. *Neve e Valanghe*, 1: 44–57 (in Italian with abstract in English) (available upon request or at: http://www.aineva.it/pubblica/neve51/6_bocchiola.html).

McClung, D. M., 2001: Extreme avalanche runout: a comparison of empirical models. *Canadian Geotechnical Journal*, 38: 1254–1265.

McClung, D. M., 2003: Magnitude and frequency of avalanches in relation to terrain and forest cover. *Arctic, Antarctic, and Alpine Research*, 35(1): 82–90.

McClung, D. M., and Mears, A. I., 1991: Extreme value prediction of snow avalanche runout. *Cold Regions Science and Technology*, 19: 163–175.

McClung, D. M., Mears, A. I., and Schaerer, P. A., 1989: Extreme avalanche run-out: data from four mountain ranges. *Annals of Glaciology*, 13: 180–184.

McLellan, B. N., and Hovey, F. W., 2001: Habitats selected by grizzly bears in a multiple use landscape. *Journal of Wildlife Management*, 65: 92–99.

Medagliani, M., Garavaglia, S., Bocchiola, D., and Rosso, R., 2007: Il bilancio idrologico dei bacini a forte contributo nivale [Hydrological balance of snow fed watersheds: the case of Mallero river]. *L'ACQUA*, No. 3, 9–20 (in Italian with abstract in English) (reprints available upon request).

Muntán, E., Andreu, L., Oller, P., Gutiérrez, E., and Martínez, P., 2004: Dendrochronological study of the Canal del Roc Roig avalanche path: first results of the Aludex project in the Pyrenees. *Annals of Glaciology*, 38(1): 173–179.

Naaim, M., Faug, T., and Naaim-Bouvet, F., 2003: Dry granular flow modelling including erosion and deposition. *Surveys in Geophysics*, 24(5): 569–585.

Naaim, M., Naaim-Bouvet, F., Faug, T., and Bouchet, A., 2004: Dense snow avalanche modelling: flow, erosion, deposition and obstacle effects. *Cold Regions Science and Technology*, 39: 193–204.

Pagani, A., and Sala, G., 2007: Simulazione di fenomeni valanghivi per la valutazione delle aree soggette a rischio: il caso del monte Vallecetta (SO) [Simulation of snow avalanches for hazard mapping: the case study of the Vallecetta mountain (SO)]. Master thesis. Politecnico di Milano, Italy (available upon request to D. Bocchiola).

Patten, R. S., and Knight, D. H., 1994: Snow avalanches and vegetation pattern in Cascade Canyon, Grand Teton National Park, Wyoming, U.S.A. *Arctic, Antarctic, and Alpine Research*, 26(1): 35–41.

Perla, R. I., Cheng, T. T., and McClung, D. M., 1980: A two-parameter model of snow-avalanche motion. *Journal of Glaciology*, 26(94): 197–207.

Rahman, A., Weinmann, P. E., Hoang, T. M. T., and Laurenson, E. M., 2002: MonteCarlo simulation of flood frequency curves from rainfall. *Journal of Hydrology*, 256: 196–210.

Reardon, B. A., Pederson, G. T., Caruso, C. J., and Fagre, D. B., 2008: Spatial reconstructions and comparisons of historic snow avalanche frequency and extent using tree rings in Glacier National Park, Montana, U.S.A. *Arctic, Antarctic, and Alpine Research*, 40(1): 148–160.

Regione Lombardia, 2002: SIRVAL, Sistema Informativo Regionale VALanghe (Regional Avalanche Information System), CD. Ed. Regione Lombardia, Direzione Generale Territorio ed Urbanistica, Milano (in Italian).

Riboni, A., Sovilla, B., Bocchiola, D., and Rosso, R., 2005: Altezza al distacco delle valanghe: un approccio regionale [The avalanche depth at release: a regional approach]. *Neve e Valanghe*, 55: 22–39 (in Italian, with abstract in English) (available upon request or at: http://www.aineva.it/pubblica/neve55/3_bocchiola.html).

Rulli, M. C., and Rosso, R., 2002: An integrated simulation method for flash-flood risk assessment: 1. Frequency predictions in the Bisagno River by combining stochastic and deterministic methods. *Hydrology and Earth System Sciences*, 6: 267–283.

Rulli, M. C., and Rosso, R., 2005: Modelling catchment erosion after wildfires in the San Gabriel Mountains of southern California. *Geophysical Research Letters*, 32: article L19401, doi: 10.1029/2005GL023635.

Salm, B., 2004: A short and personal history of snow avalanche dynamics. *Cold Regions Science and Technology*, 39: 83–92.

Salm, B., Burkard, A., and Gubler, H., 1990: Berechnung von Fliesslawinen: eine Anleitung für Praktiker mit Beispielen [Avalanche calculations: a practical method with examples]. Eidgenössische Institut für Schnee und Lawinenforschung, SLF Davos, Switzerland, Mitteilungen n. 47, 41 pp. (in German).

Salvadori, G., and De Michele, C., 2006: Statistical characterization of temporal structure of storms. *Advances in Water Resources*, 29: 827–842.

Schaerer, P. A., 1988: The yield of avalanche snow at Rogers pass, British Columbia, Canada. *Journal of Glaciology*, 34(117): 188–193.

Schrott, L., Hufschmidt, G., Hankammer, M., Hoffmann, T., and Dikau, R., 2003: Spatial distribution of sediment storage types and quantification of valley fill deposits in an alpine basin, Reintal, Bavarian Alps, Germany. *Geomorphology*, 55: 45–63.

Skaugen, T., 1999: Estimating the mean areal snow water equivalent by integration in time and space. *Hydrological Processes*, 13: 2051–2066.

Smith, D. J., McCarthy, D. P., and Luckman, B. H., 1994: Snow-avalanche impact pools in the Canadian Rocky Mountains. *Arctic, Antarctic, and Alpine Research*, 26(2): 116–127.

Smith, M. J., and McClung, D. M., 1997: Characteristics and prediction of high-frequency avalanche runout. *Arctic, Antarctic, and Alpine Research*, 29(3): 352–357.

Sovilla, B., 2002: Parametri di input per simulazioni di valanghe dense [Input parameters for dense snow avalanches simulation]. Course on avalanche dynamics, Eidgenössische Institut für Schnee und Lawinenforschung, SLF Davos, held in Bormio, 4–5 December (in Italian).

Sovilla, B., 2004: Field experiments and numerical modelling of mass entrainment and deposition processes in snow avalanches. PhD thesis No. 15462. ETH Zurich, Switzerland (available at: http://www.slf.ch/staff/pers-home/sovilla/sovilla-en.html).

Sovilla, B., and Bartelt, P., 2002: Observations and modelling of snow avalanche entrainment. *Natural Hazards*, 2: 169–179.

Sovilla, B., Burlando, P., and Bartelt, P., 2006: Field experiments and numerical modelling of mass entrainment in snow avalanches. *Journal of Geophysical Research*, 111: article F03007, doi: 10:1029/2005JF000391.

Sovilla, B., Margreth, S., and Bartelt, P., 2007: On snow entrainment in avalanche dynamics calculations. *Cold Regions Science and Technology*, 47: 69–79.

Veblen, T. T., Hadley, K. S., Nel, E. M., Kitzberger, T., Reid, M., and Villalba, R., 1994: Disturbance regime and disturbance interactions in a Rocky Mountain subalpine forest. *Journal of Ecology*, 82: 125–135.

Veneziano, D., Iacobellis, V. P., and Furcolo, P., 2002: Multifractality of iterated pulse processes with pulse amplitudes generated by a random cascade. *Fractals*, 10(2): 209–222.

Voellmy, A., 1955: Über die Zerstörungskraft von lawinen [About the destructive force of avalanches]. *Schwerizerische Bauzeitung, Jahrgang*, 73.

Wagnon, P., Linda, A., Arnaud, Y., Kumar, R., Sharma, P., Vincent, C., Pottakkal, J. G., Berthier, E., Ramanathan, A., Hasnain, S. I., and Chevallier, P., 2007: Four years of mass balance on Chhota Shigri Glacier, Himachal Pradesh, India, a new benchmark glacier in the western Himalaya. *Journal of Glaciology*, 53(183): 603–611.

Wilby, R. L., and Wigley, T. M. L., 2002: Future changes in the distribution of daily precipitation totals across North America. *Geophysical Research Letters*, 29(7): 1135, doi: 10.1029/2001gl013048.

MS accepted January 2009